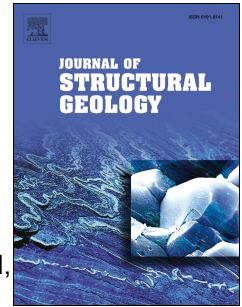


Accepted Manuscript

Two-stage terrane assembly in Western Gondwana: Insights from structural geology and geophysical data of central Borborema Province, NE Brazil

Lauro Cézar M. de Lira Santos, Elton L. Dantas, Roberta M. Vidotti, Peter A. Cawood, Edilton J. dos Santos, Reinhadt A. Fuck, Haroldo M. Lima



PII: S0191-8141(17)30185-2

DOI: [10.1016/j.jsg.2017.09.012](https://doi.org/10.1016/j.jsg.2017.09.012)

Reference: SG 3530

To appear in: *Journal of Structural Geology*

Received Date: 31 March 2017

Revised Date: 3 September 2017

Accepted Date: 17 September 2017

Please cite this article as: de Lira Santos, Lauro.Cé.M., Dantas, E.L., Vidotti, R.M., Cawood, P.A., dos Santos, E.J., Fuck, R.A., Lima, H.M., Two-stage terrane assembly in Western Gondwana: Insights from structural geology and geophysical data of central Borborema Province, NE Brazil, *Journal of Structural Geology* (2017), doi: 10.1016/j.jsg.2017.09.012.

This is a PDF file of an unedited manuscript that has been accepted for publication. As a service to our customers we are providing this early version of the manuscript. The manuscript will undergo copyediting, typesetting, and review of the resulting proof before it is published in its final form. Please note that during the production process errors may be discovered which could affect the content, and all legal disclaimers that apply to the journal pertain.

1 **TWO-STAGE TERRANE ASSEMBLY IN WESTERN GONDWANA:**
2 **INSIGHTS FROM STRUCTURAL GEOLOGY AND GEOPHYSICAL DATA**
3 **OF CENTRAL BORBOREMA PROVINCE, NE BRAZIL.**

4 Lauro César M. de Lira Santos^{1,2,*}; Elton L. Dantas¹; Roberta M. Vidotti¹ Peter A.
5 Cawood^{3,4}; Edilton J. dos Santos⁵, Reinhardt A. Fuck¹, Haroldo M. Lima¹

6 ¹Instituto de Geociências, Universidade de Brasília, Brazil; ²Unidade Acadêmica de
7 Mineração e Geologia, Universidade Federal de Campina Grande, Brazil; ³School of
8 Earth, Atmosphere and Environment, Monash University, Victoria 3800, Australia;
9 ⁴Department of Earth Sciences, University of St Andrews, St Andrews KY16 9AL, UK.
10 ⁵Serviço Geológico do Brasil - CPRM, Brazil.

11 **Postal and e-mail addresses:**

12 ¹Campus Universitário Darcy Ribeiro, 70910-900, Brasília-DF, Brazil:
13 *lauromontefalco@gmail.com;* *elton@unb.br;* *roberta@unb.br;*
14 *haroldogeologo@gmail.com;* ²Aprigio Veloso Street - 882, 58429140, Campina
15 Grande-PB, Brazil; ³Melbourne, VIC 3800, Australia: *peter.cawood@monash.edu;*
16 ⁵South Avenue - 2291, 50770011, Recife-PE, Brazil: *edilton.santos@cprm.gov.br;*

17

18 *Corresponding author, E-mail: *lauromontefalco@gmail.com;* Phones: +55 83
19 996770861, + 55 83 30886129;

20 **Keywords:** Polycyclic deformation, Western Gondwana, Borborema Province,
21 Accretion tectonics.

22

23

24

25

26

27

28 ABSTRACT

29 Combined geophysical and structural data from the Transversal Subprovince of the
30 Borborema Province (NE Brazil) highlight the internal structure of, and
31 interrelationships between, the constituent terranes. Radiometric and magnetic maps
32 show distinctive signatures for the Archean-Paleoproterozoic Alto Moxotó and Meso-
33 to Neoproterozoic Alto Pajeú and Pernambuco-Alagoas terranes. Mapped radiometric
34 and first and second order magnetic lineaments, associated with Euler deconvolution,
35 enable correlation between geophysical data and major structures. In addition to early
36 related deformation of the Alto Moxotó Terrane, combined analysis of late transposition
37 foliations, lineations and kinematic criteria reveal a complex structural evolution
38 marked by two distinct assembly stages. The first phase is characterized by thrust
39 tectonics with top-to-the-south vergence, resulting in the juxtaposition of the
40 allochthonous Alto Pajeú Terrane with the structurally underlying Alto Moxotó Terrane.
41 The terrane boundary is delineated by the Serra de Jabitacá Shear Zone, which is
42 associated with low dipping collisional granitic sheets and ca. 1.0 Ga mafic-ultramafic
43 rocks interpreted as obducted ophiolite remnants. Later strike-slip movements strongly
44 folded and obliterated thrust-related markers, and the continental scale E-W
45 Pernambuco Lineament is interpreted as the result of lateral assembly between the
46 composite Alto Pajeú-Alto Moxotó terranes and the Pernambuco-Alagoas Terrane
47 during the metamorphic peak of the Brasiliano orogeny. Evolution of the Borborema
48 Province reflects accretionary processes during the assembly of Western Gondwana.

49

50 **1. Introduction**

51 Orogenic belts develop through convergent and collisional episodes of plate
52 interaction, resulting in areas of strong regional deformation. Despite the unique internal
53 architecture of each orogen, they can be classified into three major end members, which
54 are often temporally connected: accretionary, collisional and intracratonic (Cawood et
55 al., 2009 and references therein). Crustal accretion in orogens occurs through frontal,
56 lateral or oblique plate motions (Colpron and Nelson, 2009; Cawood et al., 2011a;
57 Tetreault and Builger, 2012). The final result is a complex mosaic of folds, thrust faults,
58 and strike-slip shear zones formed in response to a strong component of crustal
59 shortening. Examples include the Appalachian-Caledonian and the Himalayan chains
60 that resulted in the closure of the Iapetus and Tethys oceans respectively, followed by a
61 final stage of continent-continent collision. In addition, frontal subduction may be
62 subsequently followed by major lateral displacements via strike-slip shear zones,
63 obliterating or overprinting early deformation stages, such as in the North America
64 Cordillera and Terra Australis orogens (Dickinson et al., 2004; Cawood et al., 2011b).

65 Tectono-stratigraphic terranes are an important component of the orogenic
66 architecture and represent fault-bounded crustal blocks with geological histories distinct
67 from adjoining blocks (Coney et al., 1980). In Western Gondwana, it is assumed that
68 convergent plate motions resulted in systematic terrane accretion events, which in the
69 South American and West African mobile belts are mostly related to the Neoproterozoic
70 Brasiliano-Pan African orogeny (Caby et al., 2003; de Wit et al., 2008; Brito Neves et
71 al., 2014). Among major Western Gondwana orogens, the Borborema Province (NE
72 Brazil) is characterized by a complex array of deformation, magmatic and metamorphic
73 events spanning almost all the Precambrian. The province is connected to Africa by
74 major lineaments and suture zones, constituting a key region to investigate major
75 geodynamic processes of Western Gondwana assembly. For instance, accretionary
76 episodes within the Borborema Province are constrained by geochronological and
77 geophysical data as shown by Brito Neves et al., 2000; Van Schmus et al., 2008; Santos
78 et al., 2010; Lages and Dantas, 2016 and Padilha et al., 2016. However, the nature and
79 kinematics of terrane assembly are poorly understood. In addition, as in other provinces
80 of Gondwana, recent studies has given major emphasis on the role of intracontinental
81 deformation, challenging the Neoproterozoic terrane accretion model (e.g. Neves et al.,
82 2017).

83 In this paper, we combine airborne geophysical data (radiometry and
84 magnetometry) and structural analysis of part of the Alto Pajeú, Alto Moxotó and
85 Pernambuco-Alagoas terranes of the central portion of the Borborema Province. Our
86 goal is to unravel the structural architecture of these domains, including the role of the
87 major shear zones that bound and internally disrupt the terranes, as well as resolving the
88 sequence of tectonic events that they have experienced. We aim to demonstrate the
89 significance of integrating geophysics and field geology to understand episodes of
90 terrane development and assembly in the region and to provide a model for unravelling
91 the development of other Precambrian polydeformed orogens.

92

93 **2. Geological Setting**

94 2.1. Borborema Province

95 The Borborema Province constitutes the northeastern portion of the Precambrian
96 platform of South American (Almeida et al., 1981). It can be traced into West Africa

97 through Benin, Nigeria and Cameroon and is located in the central part of Western
98 Gondwana (Fig. 1; Trompette, 1994; Van Schmus et al., 2008). The province is
99 bounded to the south by the São Francisco Craton, to the west by the Parnaíba Basin,
100 and to the north and east by marginal basins, comprising highly deformed and
101 frequently migmatized Paleoproterozoic terranes, locally including Archean fragments
102 (Brito Neves et al., 2000; Fetter et al., 2000; Dantas et al., 2013). Such terranes are
103 interleaved with early to late Neoproterozoic terranes, forming mobile belts with
104 widespread metamorphosed volcanosedimentary (mostly metapelitic) sequences (Van
105 Schmus et al., 2003; Hollanda et al., 2015) and remnants of Ediacaran continental
106 magmatic arcs (Fetter et al., 2003; Araújo et al., 2014, Brito Neves et al., 2014). Several
107 major shear zones transect the Bordorema Province (e.g., Transbrasiliiano-Kandhi
108 lineament) and separate major domains, with the E-W trending Patos and Pernambuco
109 dextral shear zones, dividing the Northern, Central and Southern Subprovinces.
110 Available Ar-Ar thermo-chronological determinations and U-Pb data indicate that
111 deformation occurred between 590 and 500 Ma (Monié et al., 1997; Corsini et al., 1998;
112 Neves et al., 2008, among others). The province is thought to have undergone a
113 polycyclic Neoproterozoic history of accretion and collision-related events (Van
114 Schmus et al., 1995, 2011; Brito Neves et al., 2000, 2014; Santos et al., 2000). This is
115 similar to the history inferred for the provinces African counterpart, along the Trans-
116 Saharan belt between the Hoggar Shield and Benin-Nigerian Province (Black et al.,
117 1994; Dawāi et al., 2017). An alternative model, argues that the province corresponds to
118 an intracontinental orogen consolidated in response to Neoproterozoic far-field stresses
119 (Neves, 2015).

120 The Northern Subprovince is divided into composite terranes surrounded by
121 supracrustal rocks as well as magmatic arcs containing Archean to Neoproterozoic
122 lithotectonic successions. The Transversal Subprovince is divided into five terranes: São
123 José do Caiano, Piancó-Alto Brígida, Alto Pajeú, Alto Moxotó and Rio Capibaribe. The
124 Southern Subprovince contains the Meso-Neoproterozoic Pernambuco-Alagoas
125 Terrane, as well as Neoproterozoic mobile belts that surround the São Francisco Craton
126 (Santos and Medeiros, 1999; Brito Neves et al., 2000).

127 The studied terranes are bounded by the Serra de Jabitacá Thrust system in the
128 north and Pernambuco Lineament in the south. The former separates the Tonian Alto
129 Pajeú Terrane (also referred to as the Cariris Velhos orogen) and the Archean-

130 Paleoproterozoic Alto Moxotó Terrane. The Pernambuco Lineament can be traced for
131 almost 700 km and is correlated with the Adamoua Lineament in NW Africa. It displays
132 dextral shear criteria and HT- and LT-mylonitic fabrics associated with Ediacaran
133 granitic plutons (Davison et al., 1995; Neves and Mariano, 1999). The contrasting
134 geological evolution on either side of this structure, the association with calc-alkaline
135 arc-related magmas and the high strain conditions has led some authors, including
136 Santos, (1996); Brito Neves et al., (2000) to consider it as a major crustal boundary.
137 This interpretation is also supported by different geophysical potential methods
138 (Oliveira, 2008; Lima et al., 2015; Santos et al., 2014).

139

140 Fig. 1 - Around Here.

141

142 2.1.1. Alto Pajeú Terrane

143 The overall northeast-southwest trending Alto Pajeú Terrane is separated from
144 the Piancó-Alto Brígida Terrane to the northwest by the NE-SW strike-slip Serra do
145 Caboclo sinistral shear zone, and from the Alto Moxotó Terrane to the southeast by the
146 poorly-defined Serra de Jabitacá thrust system (Santos and Medeiros, 1999, Fig. 2). The
147 terrane is characterized by calc-alkaline and peraluminous Tonian granites with arc-
148 related to syn-collisional geochemical signatures, metamafic rocks and metaultramafic
149 rocks, including remnants of ophiolites and deep-arc roots (Serrote das Pedras Pretas
150 Suite). It also includes pelitic metasedimentary and meta-volcanoclastic rocks of the São
151 Caetano Complex that are interpreted to have formed in a back arc basin environment
152 (Brito Neves et al., 1995; Santos, 1995; Lages and Dantas, 2016). The terrane is the
153 type area for the Cariris Velhos orogeny (ca. 1.0-0.96 Ga, Kozuch, 2003; Santos et al.,
154 2010). Paleoproterozoic crust is largely absent from the Alto Pajeú Terrane, which is
155 abundant in the adjoining Alto Moxotó Terrane. Similar assemblages also occur in other
156 parts of the province (Carvalho, 2005; Oliveira et al., 2010; Caxito et al., 2014a).
157 Furthermore, Ediacaran granites are widespread and cross-cut the main supracrustal
158 associations of the Cariris Velhos orogen, including the Serra do Arapuá, Riacho do Icó,
159 and Quixaba plutons (Santos, 1995; Santos and Medeiros, 1999).

160

161 *2.1.2. Alto Moxotó Terrane*

162 The Alto Moxotó Terrane corresponds to a high-grade metamorphic crustal
163 block composed of orthogneisses, migmatites and metagranites (Floresta Suite), mafic-
164 ultramafic rocks (Malhada Vermelha or Carmo Suites) and supracrustal sequences
165 (Sertânia Complex) that experienced accretion and collision events between ca. 2.4 to
166 2.0 Ga (Fig. 2; Santos et al., 2004; Santos et al., 2015a). It records a major eclogite to
167 granulite facies metamorphic peak at ca. 1.9 Ga (Neves et al. 2015). Its boundary with
168 the Southern Subprovince is the E-W continental scale dextral strike-slip Pernambuco
169 Lineament (Fig. 2).

170 Santos et al., (2015b) have recently documented Neoproterozoic TTG rocks (Riacho
171 das Lajes Suite) in the inner portion of the terrane, which are unique within the
172 Transversal Subprovince. Furthermore, the terrane lacks evidence for the Cariris Velhos
173 and Brasiliano orogenic events, but does contain minor occurrences of Cambrian A-type
174 granites along its margins (Guimarães et al., 2005). Such features led several authors,
175 including Brito Neves et al., (2000) and Santos et al., (2004) to consider this domain as
176 an exotic Paleoproterozoic fragment within the Neoproterozoic Transversal
177 Subprovince.

178

179 *2.1.3. Pernambuco-Alagoas Terrane*

180 The Pernambuco-Alagoas Terrane occupies the northern portion of the Southern
181 Subprovince. The southern limit of this terrane is defined by the Belo Monte Jeremoabo
182 Shear Zone (Brito Neves et al., 2000). The main geological units of the terrane range in
183 age from ca. 1.13 to 0.96 Ga and are represented by the Cabrobó supracrustal sequence,
184 which includes paragneisses, metagraywackes and calc-silicate rocks, and the Belém do
185 São Francisco Complex, composed of granitic to granodioritic banded orthogneisses
186 and migmatites (Fig. 2; Silva Filho et al., 2010 and references therein).

187 The structural framework of the terrane is interpreted as the result of intense
188 Brasiliano-related deformation overprinting a Tonian fabric. One of the most important
189 characteristics is the widespread occurrence of Ediacaran to Cambrian granitic
190 intrusions, which are completely absent in the adjacent Alto Moxotó Terrane. These
191 include mainly high-K calc-alkaline to shoshonitic batholiths, which has been recently

192 grouped as Buíque-Paulo Afonso, Águas Belas-Canindé, Maribondo-Correntes and
193 Ipojuca-Atalaia (Silva Filho et al., 2010), as well as minor bodies like the Fortuna
194 intrusion, which are interleaved with Paleoproterozoic supracrustal sequences (Silva
195 Filho et al., 2014). Such granitic rocks mark the development and evolution of a
196 continental arc during the Brasiliano orogeny. Recently, local occurrences of Archean
197 rocks has also been described in the westernmost portion of this terrane (Cruz et al.,
198 2015).

199

200 Fig. 2 - Around Here.

201

202 3. Geophysical dataset

203 Airborne radiometric and magnetic data for the study area were obtained from
204 the Pernambuco-Paraíba and Paraíba-Rio Grande do Norte projects undertaken by the
205 Geological Survey of Brazil (CPRM) in 2010 that cover an area of 134.644,89 km².
206 These data were used to identify anomalies, delimit areas of contrasting geophysical
207 character, and define lineaments within and between terranes (Fig. 3).

208 The N-S-trending flight lines were spaced at 0.5 km, whereas E-W tie lines were
209 spaced at 10 km. The nominal flight height and speed were 100 m and 270 km/h,
210 respectively (LASA and Proscpectors, 2010), and sampling intervals were 1 s for the
211 gamma spectrometer and 0.1 s for magnetometer. Geophysical data were processed with
212 the GEOSOFT Oasis Montaj 8.0 at the University of Brasília.

213 Total count (TC), eTh/K ratio as well as RGB (RGB = red, green and blue)
214 ternary composition maps were created using the gamma-ray spectrometric data to
215 delimit compositional variations across the study area (Jacques et al., 1997). For
216 analysis of magnetic data, we used the Magnetic anomaly (MA), First Vertical
217 Derivative (DV), Total Gradient (TG) and Tilt Derivative (TDR). The total gradient is
218 suitable for identification of the borders of magnetic bodies in regions of low latitude
219 and in the presence of significant remanence when sources of interest are shallow or
220 very regional (Li, 2006; Isles and Rankin, 2013). Tilt derivative (Miller and Singh,
221 1994) was applied to enhance the edges of magnetic sources related to geological
222 contacts and structural fabric.

223

224 Fig. 3 - Around Here.

225

226 **4 Results**

227 4.1. Gamma ray spectrometric data

228 Interpretation of radiometric data was based on the distribution of the
229 radioelements in order to define major contrasts between the studied terranes. All
230 channels (K, eTh and eU) were used to obtain general information about the study area
231 (not shown), but with major emphasis given to the Total Count (TC), eTh/K ratio and
232 composite RGB (Figs. 4 and 5). The TC map was used to define a total of 11
233 radiometric domains (A to K), which are closely associated to the major mapped
234 geologic units (Fig. 2). The strong correlation between radiometric and field geological
235 data reflects the low relief and scarce vegetation cover in the study area. Major and
236 secondary lineaments, were identified on the basis of trends in the radiometric data.

237 The Alto Pajeú Terrane comprises the majority of identified radiometric
238 domains. Domains A and B are characterized by moderate to strong K values, which
239 correspond to the Brasiliano plutonic suites; the Riacho do Icó suite has granodioritic to
240 granitic composition, whereas Quixaba and Serra do Arapuá suites correspond to
241 monzo- to syenogranites. Domain C corresponds to a northeast elongated body with
242 slight enrichment of K values, and correlates with the Cariris Velhos metagranites.
243 Domain D is characterized by intermediate concentration of radionuclides (Figs. 4a and
244 4b). This signature can be attributed to supracrustal rocks, specifically muscovite-
245 schists and intermediate metavolcanic rocks of the São Caetano Complex. In this
246 terrane, Domain I corresponds to a local, discontinuous, poorly mapped Phanerozoic
247 cover which has a very similar pattern to the Jatobá Basin in the SE portion of the study
248 area. In addition, the gamma-ray spectrometric map of the Alto Pajeú Terrane is
249 characterized by the alternation of low and high contents of radionuclides (Fig. 5a). The
250 rock heterogeneity within the Alto Pajeú Terrane is reflected in values ranging from low
251 to high on the TC map (6.9 to 28.5 $\mu\text{R/h}$). Low to moderate values are attributed to
252 supracrustal rocks of the São Caetano Complex, whereas higher values record the
253 signature of Brasiliano granitoids. This correlation is consistent with the distribution of

254 eTh/K values (Fig. 5b). Radiometric-defined lineaments are mostly oriented in the NE-
255 SW direction (Figs. 5c and 5d).

256 The Alto Moxotó Terrane presents a heterogeneous distribution of
257 radionuclides, recorded by domains E, F, G and H (Figs. 4a and 4b). E domain is
258 characterized by intermediate eU and eTh compositions, and corresponds to highly
259 deformed monzogranitic gneisses, possibly enriched in monazite. F domain is
260 represented by enrichment in eTh as compared to the other radionuclides, which is
261 attributed to the Archean tonalitic, trondhjemitic and granodioritic rocks of the Riacho
262 das Lages Suite. The G domain displays an intermediate distribution of K, eTh and eU,
263 and is associated with metagraywackes, paragneisses and migmatites of the Sertânia
264 Complex. Domain H has low values of radionuclides, where TC is around 6.9 $\mu\text{R}/\text{h}$
265 (Fig. 5a), reflecting the dioritic to granodioritic Floresta Suite as well as intercalated
266 mafic bodies of the Malhada Vermelha Suite. The radiometric signature of domains E, F
267 and G marks a progressive increase of eTh/K ratio from south to north (Fig. 5b).
268 Radiometric lineaments of the Alto Moxotó Terrane are intensively folded, but in the
269 southern portion they trend largely E-W (Figs. 5c and 5d).

270 The Pernambuco-Alagoas Terrane is subdivided into radiometric domains J and
271 K. Both domains comprise metamorphic rocks of the Belém do São Francisco Complex,
272 however the more potassic signature of K domain can be related to the presence of K-
273 rich syenitic to alkali-feldspar granitoids of the Fortuna Suite (Figs. 4a and 4b). The
274 radiometric signature observed on the TC map (Fig. 5a) shows an overall relatively
275 homogeneous distribution of radionuclides, ranging from intermediate to slightly high
276 (15.8 to 21.4 $\mu\text{R}/\text{h}$). However, anomalously high values ($> 21.4 \mu\text{R}/\text{h}$) punctuate the
277 area and correlate with Brasileiro K-rich granites (Fig. 5a). In addition, the eTh/K ratio
278 map (Fig. 5b) is characterized by very low ratios (1.9 to 2.5). Within the Pernambuco-
279 Alagoas Terrane, radiometric lineaments follow a NW-SE trend (Figs. 5c and 5d).

280

281 Fig. 4 - Around Here.

282 Fig. 5 - Around Here.

283

284 4.2. Magnetic data analysis

285 Integration of MA and TG maps (Figs. 6a and 6b) enable delineation of the main
 286 magnetic domains. Combining these data with First derivative and Tilt derivative maps
 287 allowed recognition of major structural trends (Fig. 7a and 7b): first order lineaments
 288 include boundaries of magnetic domains whereas second order lineaments correspond to
 289 alignments within domains (Figs. 6c, 6d, 7c and 7d). Based on major variations of
 290 magnetic gradient values, amplitudes, reliefs and pattern of structural lineaments, we
 291 identified eleven magnetic domains (Table 1 and Fig. 8).

Interpreted magnetic domain	Terrane	Average directions of magnetic lineaments	Description
I	Alto Pajeú	N40°E and E-W	Irregular magnetic relief reflecting localized magnetic sources with associated gradients ranging from 0.013 to 0.0032 nT/m.
II	Alto Pajeú	N25°E	Slightly irregular magnetic relief and high magnetic anomalies values, ranging from 16.3 to 56.9 nT (Fig. 6a) with intermediate to high gradients (0.032 to 0.300 nT/m).
III	Alto Pajeú	N65°E and S80°E	Very low magnetic anomalies, ranging between 17.6 and -75.1 nT. Average magnetic gradients are 0.300 nT/m.
IV	Alto Pajeú	E-W and N75°E	Rugged magnetic pattern, considerably high magnetic intensity (> 45.7 nT) and high gradients (0.200 nT/m).
V	Alto Moxotó	N42°E	Rugged magnetic pattern and a curvilinear shape with high magnetic intensities (16.3 to 38.1 nT).
VI	Alto Moxotó	N65°E	Elongated and folded shape, being characterized by high magnetic values (16.3 to 38.9 nT) and low gradients (0.016 to 0.032 nT/m).
VII	Alto Moxotó	N35°E, N75°E, E-W and N-S	Rugged magnetic relief with mostly negative magnetic anomalies (-26.5 to

			11.8 nT). Gradients are mostly low (0.016 to 0.023 nT/m), excepted to localized higher values.
VIII	Alto Moxotó	E-W	Very low magnetic anomaly values (around -75.1 nT) and high gradients (> 0.153 nT/m).
IX	Pernambuco-Alagoas	E-W and N45°W	Low magnetic expression (-45.9 nT), except for local magnetic peaks. High gradients ranging from 0.054 to 0.153 nT/m).
X	Pernambuco-Alagoas	N60°W	Very low magnetic intensity anomalies, ranging from -75.1 to -26.5 nT and gradients are intermediate to high (0.032 to 0.153 nT/m).
XI	Pernambuco-Alagoas	N75°W	Low to intermediate magnetic anomalies and gradients ranging from -11.8 to -16.3 nT and 0.027 to 0.045 nT/m, respectively.

292 Table 1 - Major characteristics of the interpreted magnetic domains on the TG, First and
 293 Tilt derivative maps.

294

295 Fig. 6 - Around Here.

296 Fig. 7 - Around Here.

297 Fig. 8 - Around Here.

298

299 4.2.1. Euler Deconvolution

300 In order to obtain additional information on source position and depths to
 301 residual magnetic sources, we performed Euler deconvolution (Thompson, 1982; Reid
 302 et al., 1990). In our approach, we choose a structural index of 1 and an associated
 303 window of 1250 m. Overall, the position of Euler solutions is in agreement with the
 304 location of the magnetic lineaments (Fig. 6). Four main categories of depth intervals
 305 were recognized: less than 100 m, between 100 and 300 m, between 300 and 600 m and

306 more than 600 m (Fig. 9). Depths varying from 0 to 100 m are mainly present in the
307 Alto Pajeú Terrane, but are also present to a lesser extent in the other terranes. Linear
308 features ranging from 100 to 300 m in depth are widespread in all terranes, including
309 the proposed terrane boundaries. Sources ranging from 300 to 600 m are relatively
310 scarce, and occur mostly along major lineaments in NWSE, ENE and NE-SW directions
311 in the Pernambuco-Alagoas, Alto Moxotó and Alto Pajeú terranes. Deeper solutions (>
312 600 m) in the studied terranes are concentrated in the NW region of the Alto Pajeú
313 terrane and in the central portion of the Pernambuco-Alagoas terrane. In addition,
314 deeper solutions are present along NW linear features of the Jatobá Basin.

315

316 Fig. 9 - Around Here.

317

318 4.3. Structural Analysis

319 A detailed mesoscopic and microscopic structural analysis was conducted in the
320 orthogneisses and supracrustal rocks of the study area. It was guided by lineament types
321 delineated by geophysical interpretations. On this basis we defined three categories of
322 lineaments (A-C). "A" lineaments are those that are well displayed on radiometric and
323 magnetic maps, and are confirmed by field data. "B" lineaments were only identified on
324 the magnetic products, mostly because of the Phanerozoic cover of the Jatobá Basin.
325 "C" lineaments were not identified on the geophysical maps, but were observed in the
326 field (Fig. 10). Structural markers and overprinting relationships allowed us to define
327 three ductile deformation stages: D_n , D_{n+1} and D_{n+2} , and the brittle D_{n+3} . The distribution
328 of field measurements of planar and linear fabrics as well as structural geological
329 sections are presented in Fig. 11.

330

331 Fig. 10 - Around Here.

332 Fig. 11 - Around Here.

333

334 4.3.1. Ductile deformation stages

335 Ductile deformation is responsible for the strongly penetrative planar fabric in
336 orthogneisses and supracrustal rocks. It is also responsible for the generation of
337 different tectonites, which occur associated to the first and second order lineaments
338 identified on the magnetic maps.

339 The D_n deformation corresponds to the random migmatitic fabric, and is
340 restricted to the central portion of the Alto Moxotó Terrane. Recognition of its nature as
341 well its associated kinematic markers are difficult to resolve in the field, as they are
342 partially to totally overprinted and obliterated by later structures. D_n is characterized by
343 the development of foliation planes (S_n) found in migmatitic portions of the Riacho das
344 Lajes Suite and Sertânia Complex. The associated metatexitic facies are frequently
345 folded and cross-cut by vein-like structures in zones of intense in situ anatexis. The
346 main D_n structures appears as open to tight folds in stromatic veins probably formed
347 during partial melting (Fig. 12a) with hinge lines plunging towards N-S, NE-SW and
348 NW-SE directions. Schollen and raft structures are also observed (Fig. 12b).

349 D_{n+1} structures are abundant at the contact between the Alto Pajeú and Alto
350 Moxotó terranes. They are characterized by a series of thrust surfaces that coincide with
351 first order magnetic lineaments inside D_n . The main associated rocks are proto-
352 mylonites and mylonites that develop planar and plano-linear fabrics, especially in
353 rocks of the São Caetano Complex, and Tonian Cariris Velhos metagranites in the Alto
354 Pajeú Terrane and in the Riacho do Navio, Riacho das Lajes and Floresta Suite in the
355 Alto Moxotó Terrane. We analyzed four thrust-directed shear zones, which from north
356 to the south are: Barra de Forquilha (BFSZ), Serra de Jabitacá (SJSZ), Floresta (FSZ)
357 and Airí (ASZ, Fig. 11). These structures trend mainly NE-SW and E-W forming a
358 major tectonic horse system. They are characterized by flat-lying to gently dipping S_{n+1}
359 foliation (Fig. 11; Fig. 12c), which can locally form duplex structures at map scale. The
360 foliations dip moderately to the N and NW and are associated with a stretching mineral
361 lineation (L_{n+1}) with medium to high pitch values (Fig. 12d). S_{n+1} foliation planes can be
362 truncated or folded by S_{n+2} fabrics, resulting in tight to isoclinal antiforms and synforms
363 responsible to L_{n+1} rotation. In addition, the F_{n+1} structures have close to tight interlimb
364 angles and include pygmatic folds (Fig. 13a). The latter structures might also be formed
365 by melt injections in the host rock. Kinematic criteria that include C and C' shear
366 bands, highly deformed σ -type quartz and K-feldspar porphyroclasts, indicate a top-to-
367 the-south tectonic vergence (Fig. 13b). The most deformed tectonites show an intense

368 recrystallization of the rock matrix and quartz grains (with undulose extinction, Fig.
369 13c), which in the mylonites and proto-mylonites include mica fishes (Fig. 13d).

370 D_{n+2} form the dominant structures in the study area, corresponding to the
371 majority of the first and second order magnetic lineaments. In the Alto Pajeú Terrane,
372 this event is represented by a complex network of NE-SW and E-W trending strike-slip
373 shear zones. This pattern of shear zones results in the tear drop shapes of supracrustal
374 rocks of the São Caetano Complex on the NW portion of the study area. (Fig. 7c). The
375 main related shear zones are Afogados da Ingazeira (AISZ), São Pedro (SPSZ) and
376 Carqueja (CSZ) (Fig. 11). Mesoscopic fabrics, including directional, oblique and down-
377 dip lineations indicate that the Barra da Foquilha Shear Zone (BFSZ) combines
378 elements of transcurrent and thrust stages or may represent a transpressional fabric. The
379 main regional structure of this stage is the strike-slip dextral Pernambuco Lineament
380 (PeL), which separates the Alto Moxotó and Pernambuco-Alagoas terranes. Planar-
381 linear tectonites predominate in the internal part of the Pernambuco-Alagoas Terrane.
382 They consist of local protomylonites that deform banded orthogneisses of the Belém do
383 São Francisco Complex. The main D_{n+2} fabrics of this terrane are recorded in the strike-
384 slip NW-SE trending sinistral Poço da Areia and Riacho do Boi shear zones.

385 Unlike the flat-lying S_{n+1} foliation, the S_{n+2} planar fabric is characterized by sub-
386 vertical to vertical mylonites and ultra-mylonites, as well as banded orthogneisses
387 corresponding to lateral simple shearing (Fig. 11; Fig. 14a). These rocks are frequently
388 associated with a well-developed sub-horizontal to horizontal L_{n+2} mineral stretching
389 lineation (Fig. 14b) defined by quartz + K-feldspar \pm biotite aggregates. Kinematic
390 indicators of D_{n+2} include rotated asymmetric quartz-aggregates and σ -type
391 porphyroclasts of quartz and K-feldspar, mantled quartz and feldspar σ -type sigmoids
392 and C- and C'-types shear surfaces including mica fish (Fig. 14c). The SC' dextral
393 fabric is particularly obvious in mylonites related to the Pernambuco Lineament,
394 characterized by recrystallized quartz and feldspar porphyroclasts, locally embedded in
395 an anastomosing S_{n+2} foliation. F_{n+2} folds are associated with the main shear zones,
396 including open to tight and isoclinal synforms, antiforms and overturned folds with
397 curved hinge lines. Oblique mineral stretching lineation (Fig. 14d) are also observed,
398 suggesting D_{n+1} and D_{n+2} fabrics interference or an oblique movement of D_{n+2} due to a
399 compressive component. The high strain corridors associated with major shear zones,
400 such in the Pernambuco Lineament show local development of sheath folds.

401 Fig. 12 - Around Here.

402 Fig. 13 - Around Here.

403 Fig. 14 - Around Here.

404

405 *4.3.2. Brittle deformation*

406 Brittle structures were observed only at a mesoscopic scale and include faults
407 and fractures that vary in dip from horizontal to vertical, and are usually discordant with
408 respect to the regional foliation. However, some fractures are concordant with the main
409 S_{n+2} shear zones, especially close to the Pernambuco Lineament. These structures are
410 consist of quartz veins or quartz-feldspar segregations that cross-cut the main L_{n+2}
411 mineral stretching lineation and hinge lines of S_{n+2} folds. Discordant structures are
412 represented by local strike-slip faults, some of which form conjugate shear systems, and
413 including domino patterns oriented in NE-SW and NW-SE (Fig. 15a). They are
414 characterized by fault slickensides composed of recrystallized quartz, chlorite and
415 sericite (Fig. 15b).

416

417 Fig. 15 - Around Here.

418

419 **5. Discussion**

420 Accretionary orogenic belts are major sites of crustal growth (Cawood et al.,
421 2009, 2013) and are widely described in several parts of Western Gondwana, including
422 examples of all ages. Most of them occupies its margins as those from the Tasman
423 orogenic system in Australia (Coney et al., 1990; McElhinny et al., 2003; Cawood,
424 2005) and the Argentine Precordillera in west South America (Ramos, 1988; Thomas
425 and Astini, 2003). However, the identification of terrane processes within a number of
426 the provinces of Gondwana remains a difficult task, mainly due deformation-related
427 reworking events.

428 Integration of geophysical and structural data for the Alto Pajeú, Alto Moxotó
429 and Pernambuco-Alagoas terranes of the Borborema Province constrain the structural
430 framework and evolution of this portion of Western Gondwana. Key geophysical
431 features suggest that the lithotectonic associations in the area correlate with distinct fault
432 bounded terranes that underwent subsequent amalgamation. These features include: (i)
433 distinct content of radionuclides, including eTh enrichment and K-depletion in the
434 Archean-Paleoproterozoic terrane, relative to the other terranes, which reflects the
435 primitive nature of the principal rock units as well as the absence of Brasiliano granites
436 (K-rich); and (ii) contrasting magnetic signatures between the terranes, with more
437 magnetic rocks present in the Alto Pajeú Terrane (Fig. 6a), whereas the Alto Moxotó
438 Terrane is characterized by low magnetic anomalies. Such a signature can be interpreted
439 as the presence of Tonian Fe-Ti ore occurrences, which are restricted to the former
440 terrane. In addition, the polyphase deformation history is constrained by the integration
441 of abundant interpreted radiometric and magnetic first and second order structures and
442 mapped structural markers, whereas Euler deconvolution constrains the position and
443 geometry of the top of the main magnetic anomalies.

444 In spite of the early folded foliations and migmatitic structures recognized in the
445 internal portions of the Alto Moxotó Terrane, thrust and transcurrent tectonics are
446 dominant. The Serra de Jabitacá Shear Zone is interpreted as a nappe-related terrane
447 boundary, reflecting the transported allochthonous character of the Alto Pajeú Terrane
448 with respect to the Alto Moxotó Terrane, which in the Borborema Province,
449 corresponds to an older basement domain. Furthermore, we speculate that crustal
450 shortening related to thrust deformation on both terranes, represent frontal/oblique
451 accretion resulting in a major basement-core nappe structure consistent with thick-
452 skinned tectonics similar to the accretion of island arcs and other continental fragments
453 towards the Eurasian margin (Pfiffner, 2006; Hall et al., 2008; Pubellier and Meresse,
454 2013).

455 The origin of mapped thrust belts in the Borborema Province is usually related to
456 terrane accretion during the early stages of the Brasiliano Orogeny (Brito Neves et al.,
457 2000; Rodrigues and Archanjo, 2011). However, accretion could also occur during the
458 1000-920 Ma Cariris Velhos orogeny. Evidence for this latter interpretation includes: (i)
459 mapped tectonic sheets of Tonian/Cariris Velhos low-angle dipping metagranites and
460 mylonites with top-to-the-south tectonic vergence, which has a geochemical signature

461 compatible with magmatic arc to collision-related settings (Santos, 1995; Santos et al.,
462 2010); (ii) the existence of dioritic-granitic dykes in the northern portion of the Alto
463 Pajeú Terrane that cross-cut similar thrust-related Tonian rocks, known as Minador
464 Suite, being interpreted as pre-Brasiliano (Sales et al., 2011), thus, marking a pre-
465 strike-slip and post-thrusting extensional stage; and (iii) the lack of thrust-related top-to-
466 the-south structural markers in the oldest Ediacaran granites. In addition, ca 1.0 Ga
467 rocks from the Serrote das Pedras Pretas Suite are associated with the Serra de Jabitacá
468 Shear Zone, being interpreted as a relic of obducted Cariris Velhos oceanic crust
469 (Santos, 1995; Lages and Dantas, 2016). Nevertheless, we recognize that there are no
470 available geochronological data for tangential deformation, especially in the Transversal
471 Subprovince (i.e. Ar-Ar plateau ages or U-Pb analysis on monazite), thus the exact
472 timing of frontal/oblique terrane assembly is still an open question.

473 Evidence for strike-slip tectonics is widespread in the Borborema Province. In
474 the study region, this is mainly represented by the Pernambuco Lineament that develop
475 E-W high strain corridors and strongly folds previous structures such as the Serra de
476 Jabitacá Shear Zone. Such structures consist mainly of mylonites up to several
477 kilometers wide, which in along the eastern branch of the lineament is associated with
478 several syn-tectonic granites (Vauchez et al., 1995; Weinberg et al., 2004). Nonetheless,
479 the age of transcurrent boundaries is still not clearly constrained, but overall strike-slip
480 movements in the Borborema Province are related to a metamorphic peak around ca.
481 590-560 Ma, during the Ediacaran-Cambrian Brasiliano Orogeny (Vauchez and Egydio-
482 Silva, 1992; Archanjo et al., 2008; Brito Neves et al., 2014; Viegas et al., 2014).

483 The geometry of structures in the Airí area is consistent with those reported from
484 classic accretionary orogens (e.g. Kusky and Bradley, 1999; Collins, 2002), and involve
485 initial thrust structures associated with terrane assembly followed by transcurrent
486 movements. The proposed polycyclic evolution in the Transversal Subprovince (Fig.
487 16) is also supported by recent magnetotelluric investigation of Padilha et al., (2016)
488 which suggests that the Cariris Velhos orogeny represents an important accretion
489 marker, followed by crustal remobilization during the Brasiliano event.

490 Most models of Gondwana assembly propose that its final configuration is the
491 result of multi-stage subduction and collision of cratonic blocks, small continents and
492 allochthonous terranes (Collins and Pisarevsky, 2005). Intense deformation during the

493 orogenic cycle strongly overprints early crust, hindering the precise definition of
494 assembly processes as well as paleogeographic correlations (e.g. de Wit et al., 2008).
495 Alternatively, in some provinces of Western Gondwana, intracontinental or
496 intracratonic deformation is invoked as a major process (Meira et al., 2015; Neves et al.,
497 2017). A crucial point is to precisely define the location and kinematics of major
498 boundaries, which can provide clues concerning that terranes were accreted via major
499 thrust or oblique subduction zones and/or subsequently dispersed by strike-slip
500 movements (Cawood et al., 2002). For instance, the Transbrasiliano-Kandi Lineament
501 represents a large-scale suture zone that marks a long-lived Neoproterozoic
502 deformational/accretionary history on the West Gondwana orogen (Araújo et al., 2016
503 and references therein).

504 Our results coupled with other geophysical investigations demonstrate the role
505 of major regional structures on the amalgamation of Western Gondwana (e.g., Santos et
506 al., 2014; Correa et al., 2015; Lima et al., 2015). Recently described Tonian to
507 Ediacaran ophiolitic sequences, continental magmatic arc-related granites, and high-
508 pressure to ultra-high-pressure rocks (Caxito et al., 2014b; Santos et al., 2015c; Brito
509 Neves et al., 2016 and references therein) coupled with suture zones mapped in NE
510 Brazil and counterparts in Africa (Black et al., 1994; Brito Neves et al., 2014) highlight
511 the importance of accretion tectonics in the building of this portion of Western
512 Gondwana.

513

514 Fig. 16 - Around Here.

515

516 **6. Conclusions**

517 Aeromagnetic and radiometric datasets combined with field-mapped structures
518 suggest that the central portion of the Borborema Province, NE Brazil, formed via two
519 distinct stages of terrane assembly. Evidence for polyphase deformation is constrained
520 by meso- and microscopic observations, including foliation transposition, distinct
521 orientation of lineations as well as several kinematic criteria associated with major shear
522 zones. Geophysical data show contrasting signatures for the major units of the studied
523 terranes.

524 The prominent mylonitic fabric associated with the Serra de Jabitacá Shear Zone
525 is associated with a thrust-related sense of movement between the Neoproterozoic Alto
526 Pajeú and Archean-Paleoproterozoic Alto Moxotó terranes. The age of this assembly is
527 uncertain being either i) early stages of Brasiliano convergence or ii) during the
528 development of the Cariris Velhos orogeny (ca. 1000-960 Ma) in the Early
529 Neoproterozoic, resulting in obduction of the 1.0 ophiolitic fragment of the Serrote das
530 Pedras Pretas Suite. Later strike-slip shear zones resulted in regional folding and
531 oblique to horizontal linear fabrics, such as those associated with the Pernambuco
532 Lineament, which is considered the main record of lateral to oblique assembly of the
533 composite Alto Pajeú and Alto Moxotó terranes with the Pernambuco-Alagoas Terrane
534 to the south. According to our model, this event took place during a metamorphic peak
535 of the Brasiliano orogeny (ca. 590-560 Ma), developing high strain zones and local
536 anatexites within major shear zones.

537 Lastly, taking into account our data and recent geophysical investigations in the
538 Borborema Province, we suggest that distinct phases of terrane collage might be acted
539 as building processes of Western Gondwana inner orogens during the Neoproterozoic.
540 Despite the difficulty on recognizing the role and evolutionary aspects of most crustal
541 boundaries, accretion tectonics provide a fair explanation for the juxtaposition of several
542 heterogeneous domains that are limited by regional/continental scale structures.

543

544 **7. Acknowledgements**

545 The authors are grateful for the editor(s) Cees Passchier and João Hippertt of
546 Journal of Structural Geology for their attention and care, during all stages of
547 publication. Jean-Luc Bouchez, Marcos Egydio-Silva, and an anonymous reviewer are
548 thanked for their criticism and suggestions that strongly improved the original
549 manuscript. Carlos José Archanjo is also thanked for early discussion. ELD and RAF
550 acknowledge National Council for Scientific and Technological Development (CNPq)
551 financial support through INCT Estudos Tectônicos and research fellowships. PAC was
552 supported by Australian Research Council grant FL160100168. We also thank CPRM
553 — Serviço Geológico do Brasil for providing access to geophysical data for academic
554 purposes.

555

556 **8. References**

- 557 Almeida, F.F.M., Hasui, Y., Brito Neves, B.B., Fuck, R.A. 1981. Brazilian structural
558 provinces: an introduction. *Earth Science Reviews* 18, 1-29.
- 559 Araujo, C.E.G., Cordani, G.U., Weinberg, R., Basei, M.A.S., Armstrong, R., Sato, K.
560 2014. Tracing Neoproterozoic subduction in the Borborema Province (NE- Brazil):
561 clues from U-Pb geochronology and Sr-Nd-Hf-O isotopes on granitoids and migmatites.
562 *Lithos* 202-203, 167-189.
- 563 Araújo, C.E.G., Cordani, G.U., Agbossoumounde, Y., Caby, R., Basei, M.A.S.,
564 Weinberg, R.F., Sato, K. 2016. Tightening-up NE Brazil and NW Africa connections:
565 New U-Pb/Lu-Hf zircon data of a complete plate tectonic cycle in the Dahomey belt of
566 the West Gondwana Orogen in Togo and Benin. *Precambrian Research* 276, 24-42.
- 567 Archanjo, C.J., Hollanda, M.H.B.M., Rodrigues, S.W., Brito Neves, B.B., 2008. Fabrics
568 of pre- and syntectonic granite plutons and chronology of shear zones in the Eastern
569 Borborema Province, NE Brazil. *Journal of Structural Geology* 30, 310-336.
- 570 Black, R., Liégeois, J.P., Latouche, L., Caby, R., Bertrand, J.M. 1994. Pan-african
571 displaced terranes in the Tuareg Shield (Central Sahara). *Geology* 22, 641-644.
- 572 Brito Neves, B.B., Santos, E.J., Schmus, W.R.Q., 2000. Tectonic history of the
573 Borborema Province. In: Umberto Cordani; Edson José Milani; Antonio Thomaz Filho;
574 Diogenes de Almeida Campos (Org.). *Tectonic Evolution of South America*. Rio de
575 Janeiro: 31st International Geological Congress, 151-182. Special Publication.
- 576 Brito Neves, B.B., Fuck, R.A., Pimentel, M.M. 2014. The Brasiliano collage in South
577 America: a review. *Brazilian Journal of Geology* 44, 493-518.
- 578 Caby, R. 2003. Terrane assembly and geodynamic evolution of Central-Western
579 Hoggar: a synthesis. *Journal of African Earth Sciences* 37, 133-159.
- 580 Carvalho, M.J. 2005. *Evolução tectônica do domínio Marancó-Poço Redondo: Registro*
581 *das orogêneses Cariris Velhos e Brasiliana na Faixa Sergipana, NE do Brasil.*
582 Universidade Estadual de Campinas, Campinas, 192 pp. (PhD thesis).

- 583 Cawood, P.A., Landis, C.A., Nemchin, A.A., Hada, S. 2002. Permian fragmentation,
584 accretion and subsequent translation of a low-latitude Tethyan seamount to the high-
585 latitude east Gondwana margin: evidence from detrital zircon age data. *Geological*
586 *Magazine* 139, 131-144.
- 587 Cawood, P.A. 2005. Terra Australis Orogen: Rodinia breakup and development of the
588 Pacific and Iapetus margins of Gondwana during the Neoproterozoic and Paleozoic.
589 *Earth Science Reviews* 69, 249-279.
- 590 Cawood, P.A., Kroner, A., Collins, W.J., Kusky, T.M., Mooney, W.D., Windley, B.F.
591 2009. Accretionary orogens through earth history. *Geological Society London Special*
592 *Publication* 318, 1–36.
- 593 Cawood, P. A., Leitch, E.C., Merle, R.E., Nemchin, A.A. 2011a. Orogenesis without
594 collision: Stabilizing the Terra Australis accretionary orogen, eastern Australia.
595 *Geological Society of America Bulletin* 123, 2240-2255.
- 596 Cawood, P.A., Pisarevsky, S., Leitch, E.C. 2011b. Unraveling the New England
597 Orocline, Eastern Gondwana Accretionary Margin. *Tectonics* 30, TC5002,
598 doi:10.1029/2011TC002864.
- 599 Cawood, P.A., C.J., Hawkesworth, Dhuime, B. 2013. The continental record and the
600 generation of continental crust. *GSA Bulletin* 125, 14-32.
- 601 Caxito, F.A., Ulhein, A., Dantas, E.L., 2014a. The Afeição augen-gneiss Suite and the
602 record of the Cariris Velhos Orogeny (1000-960 Ma) within the Riacho do Pontal fold
603 belt, NE Brazil. *Journal of South American Earth Sciences* 51, 12-27.
- 604 Caxito, F.A., Ulhein, A., Stevenson, R., Ulhein, G. 2014b. Neoproterozoic oceanic crust
605 remnants in northeast Brazil. *Geology* 45, 387-390.
- 606 Collins, W.J. 2002. Hot orogens, tectonic switching, and creation of continental crust.
607 *Geology* 30, 535-538.
- 608 Collins, A.S., Pisarevsky, S.A. 2005. Amalgamating eastern Gondwana: The evolution
609 of the Circum-Indian Orogens. *Earth-Science Reviews* 71, 229-270.

- 610 Colpron, M.; Nelson, J.L.; (eds) 2006. Paleozoic evolution and metallogeny of
611 Pericratonic Terranes at the Ancient Pacific Margin of North America, Canadian and
612 Alaskan Cordillera. Geological Association of Canada, Special Paper, 45.
- 613 Coney, P.J., Jones, D.L., Monger, J.W.H. 1980. Cordilleran suspect terranes. *Nature*
614 288, 329-333.
- 615 Coney, P.J., Edwards, A., Hine, W., Morrison, F., Windrim, D. 1990. The regional
616 tectonics of the Tasman orogenic system, eastern Australia. *Journal of Structural*
617 *Geology* 12, 519-543.
- 618 Correa, R.T., Vidotti, R.A., Oksum, E. 2016. Curie surface of Borborema Province,
619 Brazil. *Tectonophysics* 679, 73-87.
- 620 Corsini, M., Figueiredo, L.L., Caby, R., Féraud, G., Ruffet, H., Vauchez, A., 1998.
621 Thermal history of the Pan-African/Brasiliano Borborema Province of northeast Brazil
622 deduced from $^{40}\text{Ar}/^{39}\text{Ar}$ analysis. *Tectonophysics* 285, 103-117.
- 623 Cruz, R.F., Pimentel, M.M., Accioly, A.C.A., 2015. Provenance of metasedimentary
624 rocks of the western Pernambuco-Alagoas domain: contribution to understand the
625 Neoproterozoic tectonic evolution of the southern Borborema Province. *Journal of*
626 *South American Earth Sciences* 58, 82-99.
- 627 Dantas, E.L., Souza, Z.S., Wernick, E., Hackspacher, P.C., Martin, H., Xiadong, D., Li,
628 J.W., 2013. Crustal growth in the 3.4-2.7 Ga São José do Campestre Massif, Borborema
629 Province, NE Brazil. *Precambrian Research* 227, 12-156.
- 630 Davison, I., McCarthy, M., Powell, D., Torres, H.H.F., Santos, C.A., 1995. Laminar
631 flow in shear zones: the Pernambuco Shear Zone, NE-Brazil. *Journal of Structural*
632 *Geology* 17, 153-161.
- 633 Dawai, D., Tchameni, R., Bascou, J., Wangmene, S.A., Tchunte, Bouchez, J. 2017.
634 Microstructures and magnetic fabrics of the Ngaoundéré granite pluton (Cameroon):
635 Implications to the late-Pan-African evolution of Central Cameroon Shear Zone. *Journal*
636 *of African Earth Sciences* 129, 887-897.

- 637 de Wit, M.J., Stankiewicz, J., Reeves, C. 2008. Restoring Pan-African-Brasiliano
638 connections: more Gondwana control, less Trans-Atlantic corruption. Geological
639 Society, London, Special Publications 294, 399-412.
- 640 Dickinson, W.R. 2004. Evolution of the North American Cordillera. Annual Reviews
641 of Earth and Planetary Sciences 32:13-45.
- 642 Fetter, A.H., Van Schmus, W.R., dos Santos, T.J.S., Arthaud, M., Nogueira Neto, J.,
643 Arthaud, M. 2000. U-Pb and Sm-Nd geochronological constraints on the crustal
644 evolution and basement architecture of Ceara State, NW Borborema Province, NE
645 Brazil: implications for the existence of the Paleoproterozoic supercontinent Atlantica.
646 Revista Brasileira de Geociencias 30, 102–106.
- 647 Fetter, A.H., Santos, T.J.S., Van Schmus, W.R., Hackpacher, P.C., Brito Neves, B.B.,
648 Arthaud, M.H., Nogueira Neto, J.A., Wernick, E. 2003. Evidence for Neoproterozoic
649 continental arc magmatism in the Santa Quiteria Batholith of Ceará State, NW
650 Borborema Province, NE Brazil: implications for the assembly of West Gondwana.
651 Gondwana Research 6, 265-273.
- 652 Guimarães, I.P., Silva Filho, A.F., Melo, S.C., Macambira M.B. 2005. Petrogenesis of
653 A-Type Granitoids from the Pajeú-Paraíba Belt, Borborema Province, NE Brazil:
654 Constraints from geochemistry and isotopic composition. Gondwana Research 8, 347-
655 362.
- 656 Hall, R., van Hattum, M.C.A., Spakman, W., 2008. Impact of India-Asia collision on
657 SE Asia: the record in Borneo. Tectonophysics 451, 366-389.
- 658 Hollanda, M.H.B.M., Archanjo, C.J., Batista, J.R., Souza, L.C. 2015. Detrital zircon
659 ages and Nd isotope compositions of the Seridó and Lavras da Mangabeira basins
660 (Borborema Province, NE Brazil): Evidence for exhumation and recycling associated
661 with a major shift of sedimentary provenance. Precambrian Research 258, 186-207.
- 662 Isles, D.J., Rankin, L.R. 2013. Geological interpretation of aeromagnetic data. Perth:
663 The Australian Society of Exploration Geophysicists, 357 p.
- 664 Jaques, A.L., Wellman, P., Whitaker, A., Wyborn, D. 1997. High resolution geophysics
665 in modern geological mapping. Journal of Australian Geology and Geophysics 17, 159-
666 173.

- 667 Kozuch, M., 2003. Isotopic and trace element geochemistry of Early Neoproterozoic
668 gneissic and metavolcanic rocks in the Cariris Velhos Orogen of the Borborema
669 Province, Brazil, and their bearing tectonic setting (PhD thesis). Kansas University,
670 Lawrence, 199 pp.
- 671 Kusky, T.M., Bradley, D.C. 1999. Kinematic analysis of melange fabrics: examples and
672 applications from the McHugh Complex, Kenai Peninsula, Alaska. *Journal of Structural*
673 *Geology* 21, 1773-1796.
- 674 Lages, G.A., Dantas, E.L. 2016. Floresta and Bodocó Mafic-Ultramafic Complexes,
675 western Borborema Province, Brazil: geochemical and isotope constraints for evolution
676 of a Neoproterozoic arc environment and retro-eclogitic hosted Ti-mineralization.
677 *Precambrian Research* 280, 95-119.
- 678 Lasa and Prospectors, 2010. Projeto Aerogeofísico Paraíba-Rio Grande do Norte-
679 Paraíba. Relatório final do levantamento e processamento dos dados magnetométricos e
680 gamaespectrométricos. V. 1. CPRM, Rio de Janeiro. 389p.
- 681 Li, X. 2006. Understanding 3D analytic signal amplitude. *Geophysics* 71, 13-16. doi:
682 10.1190/1.2184367.
- 683 Lima, M.V.A.G., Berrocal, J., Soares, J.E.P., Fuck, R.A. 2015. Deep seismic refraction
684 experiment in northeast Brazil: New constraints for Borborema Province evolution.
685 *Journal of South American Earth Sciences* 58, 335-349.
- 686 McElhinny, M.W., Powell, C.M., Pisarevsky, S.A. 2003. Paleozoic terranes of eastern
687 Australia and the drift history of Gondwana. *Tectonophysics* 362, 41-65.
- 688 Meira, V.T., Garcia-Casco, A., Juliani, C., Almeida, R.P., Hans, J., Schoscher, D. 2014.
689 The role of intracontinental deformation in supercontinent assembly: insights from the
690 Ribeira Belt, Southeastern Brazil. *Terra Nova* 27, 206-217.
- 691 Miller, H.G., Singh, V. 1994. Potential field tilt - a new concept for location of potential
692 field sources. *Journal of applied Geophysics* 32, 213-217.
- 693 Monié, O., Caby, R., Arthaud, M.H. 1997. The Neoproterozoic Brasiliano orogeny in
694 northeast Brazil: $40\text{Ar}/39\text{Ar}$ and petrostructural data from Ceará. *Precambrian*
695 *Research* 81, 241-264.

- 696 Neves, S.P., Mariano, G. 1999. Assessing the tectonic significance of a large-scale
697 transcurrent shear zone system: The Pernambuco lineament, northeastern Brazil. *Journal*
698 *of Structural Geology* 21, 1369-1383.
- 699 Neves, S.P., Bruguier, O., Bosch, D., Silva, J.M.R., Mariano, G. 2008. U-Pb ages of
700 plutonic and metaplutonic rocks in the southern Borborema Province (NE Brazil):
701 timing of Brasiliano deformation and magmatism. *Journal of South American Earth*
702 *Sciences* 25, 285-297.
- 703 Neves, S.P., 2015. Constraints from zircon geochronology on the tectonic evolution of
704 the Borborema Province (NE Brazil): widespread intracontinental Neoproterozoic
705 reworking of a Paleoproterozoic accretionary orogeny. *Journal of South American*
706 *Earth Sciences* 58, 150-164.
- 707 Neves, S.P., Lages, G.A., Brasilino, R.G., Miranda, A.W.A., 2015. Paleoproterozoic
708 accretionary and collisional processes and the build-up of the Borborema Province (NE
709 Brazil): Geochronological and geochemical evidence from the Central Domain. *Journal*
710 *of South American Earth Sciences* 58, 165-187.
- 711 Neves, S.P., Silva, J.M.R., Bruguier, O. 2017. Geometry, kinematics and geochronology
712 of the Sertânia Complex (central Borborema Province, NE Brazil): Assessing the role of
713 accretionary versus intraplate processes during Wes Gondwana assembly. *Precambrian*
714 *Research* 298, 552-571.
- 715 Oliveira, R.G., 2008. Arcabouço Geofísico, Isostasia e causas do magmatismo
716 cenozóico da Província Borborema e de sua Margem Continental (NE do Brasil) (PhD
717 thesis). Universidade Federal do Rio Grande do Norte, Natal, 411 pp.
- 718 Oliveira, E.P., Windley, B.F., Araújo, M.N.C., 2010. The Neoproterozoic Sergipano
719 orogenic belt, NE Brazil: a complete plate tectonic cycle in western Gondwana.
720 *Precambrian Research* 181, 64-84.
- 721 Padilha, A.L., Vitorello, Í., Pádua, M.B., Fuck, R.A. 2016. Deep magnetotelluric
722 signatures of the early Neoproterozoic Cariris Velhos tectonic event within the
723 Transversal Sub-province of the Borborema Province, NE Brazil. *Precambrian Research*
724 275, 70-83.

- 725 Pfiffner, O.A. 2006. Thick-skinned and thin-skinned styles of continental contraction.
726 Special Paper of Geological Society of America 414, 153-177.
- 727 Pubellier, M., Meresse, F. 2013. Phanerozoic growth of Asia: Geodynamic processes
728 and evolution. *Journal of Asian Earth Sciences* 72, 118-128.
- 729 Ramos, V.A. 1998. Late Proterozoic-Early Paleozoic of South America: a collisional
730 history. *Episodes* 11, 168-174.
- 731 Reid, A.B., Allson, J.M., Granser, H., Mielt, A.J., Somerton, I.W. 1990. Magnetic
732 interpretation in three dimensions using Euler deconvolution. *Geophysics* 55, 80-91.
- 733 Rodrigues, S.W.O., Archanjo, C.J. 2011. Estruturas e histórias deformacionais
734 contrastantes dos granitos sintectônicos de Campina Grande e Serra Redonda, Província
735 Borborema, NE do Brazil. *Geologia USP - Série Científica* 11, 3-17.
- 736 Sales, A.O., Santos, E.J., Lima, E.S., Santos, L.C.M.L., Brito Neves, B.B.B. 2011.
737 Evolução petrogenética e tectônica do Evento Cariris Velhos na região de Afogados da
738 Ingazeira (PE), Terreno Alto Pajeú, Província Borborema. *Geologia USP - Série*
739 *Científica* 11, 101-121.
- 740 Santos, A.C.L., Padilha, A.L., Fuck, R.A., Pires, A.C.B., Vitorello, I., Pádua, M.B.
741 2014. Deep structure of a stretched lithosphere: Magnetotelluric imaging of the
742 southeastern Borborema Province, NE Brazil. *Tectonophysics* 610, 39-50.
- 743 Santos, E.J., 1995. O complexo granítico Lagoa das Pedras: acreção e colisão na região
744 de Floresta (Pernambuco), Província Borborema (PhD thesis). Instituto de Geociências
745 da Universidade de São Paulo, São Paulo, 228 pp.
- 746 Santos, E.J., Medeiros, V.C., 1999. Constraints from granitic plutonism on Proterozoic
747 crustal growth of the Transverse Zone, Borborema Province, NE-Brazil. *Revista*
748 *Brasileira de Geociências* 29, 73-84.
- 749 Santos, E.J., Brito Neves, B.B., Van Schmus, W.R., Oliveira, R.G., Medeiros, V.C.,
750 2000. An overall view on the displaced terrane arrangement of the Borborema Province,
751 NE Brazil. In: *International Geological Congress, 31th, Rio de Janeiro, Brazil, General*
752 *Symposia, Tectonic Evolution of South American Platform*, 5-9.

- 753 Santos, E.J., Nutman, A.P., Brito Neves, B.B., 2004. Idades SHRIMP U-Pb do
754 Complexo Sertânia: implicações sobre a evolução tectônica da Zona Transversal,
755 Província Borborema. *Geologia USP - Série Científica* 4, 1-12.
- 756 Santos, E.J., Van Schmus, W.R., Kozuch, M., Brito Neves, B.B., 2010. The Cariris
757 Velhos tectonic event in northeast Brazil. *J. South American. Earth Sciences.* 29, 61-76.
- 758 Santos, L.C.M.L., Dantas, E.L., Santos, E.J., Santos, R.V., Lima, H.M., 2015a. Early to
759 late Paleoproterozoic magmatism in NE Brazil: the Alto Moxoto Terrane and its
760 tectonic implications for the pre-Western Gondwana assembly. *Journal of South*
761 *American Earth Sciences.* 58, 188-209.
- 762 Santos, L.C.M.L., Dantas, E.L., Santos, E.J., Fuck, R.A. 2015b. A Suíte Riacho das
763 Lajes como registro de crescimento crustal Neoarqueano no Terreno Alto Moxotó da
764 Província Borborema (NE do Brasil). In: XV Congresso Brasileiro de Geoquímica,
765 Brasília, Brazil.
- 766 Santos, T.J.S., Amaral, W.S., Ancelmi, M.F., Pitarello, M.Z., Fuck, R.A., Dantas, E.L.,
767 2015c. U-Pb age of the coesite-bearing eclogite from NW Borborema Province, NE
768 Brazil: Implications for western Gondwana assembly. *Gondwana Research* 28, 1183-
769 1196.
- 770 Silva Filho, A.F., Guimarães, I.P., Ferreira, V.P., Armstrong, R., Sial, A.N. 2010.
771 Ediacaran Águas Belas pluton, Northeastern Brazil. Evidence on age emplacement.
772 *Gondwana Research* 17, 676-687.
- 773 Silva Filho, A.F., Guimarães, I.P., Van Schmus, W.R., Armstrong, R., Silva, J.M.R.,
774 Osako, L., Concentino, L., Lima, D., 2014. SHRIMP U-Pb zircon geochronology and
775 Nd signatures of supracrustal sequences and orthogneisses constrain the Neoproterozoic
776 evolution of the Pernambuco-Alagoas domain, southern part of the Borborema
777 Province, NE Brazil. *International Journal of Earth Sciences* 21, 2155-2190.
- 778 Tetreault, J.L., Buiter, S.J.H. 2012. Geodynamic models of terrane accretion: Testing
779 the fate of island arcs, oceanic plateaus, and continental fragments in subduction zones.
780 *Journal of Geophysical Research* 117, 1-12.
- 781 Thomas, W.A., Astini, R.A. 2003. Ordovician accretion of the Argentine Precordillera
782 terrane to Gondwana: a review. *Journal of South American Earth Sciences* 16, 67-79.

- 783 Thompson, D.T. 1982. EULDPH: a new technique for making computer assisted depth
784 estimate from magnetic data. *Geophysics* 47, 31-37.
- 785 Trompette, R., 1994. *Geology of Western Gondwana, Pan-African-Brasiliano*
786 *Aggregation of South America and Africa*. A.A. Balkema, Rotterdam, p. 350.
- 787 Van Schmus, W.R., Brito Neves, B.B., Hackspacher, P.C., Babinski, M., 1995. U/Pb
788 and Sm/Nd geochronologic studies of the eastern Borborema Province, Northeast
789 Brazil: initial conclusions. *Journal of South American Earth Sciences* 8, 267-288.
- 790 Van Schmus, W.R., Brito Neves, B.B., Williams, I.S., Hackspacher, P., Fetter, A.H.,
791 Dantas, E.L., Babinski, M. 2003. The Seridó Group of NE Brazil, a late Neoproterozoic
792 pre- to syn-collisional basin in West Gondwana: insights from SHRIMP U-Pb detrital
793 zircon ages and Sm-Nd crustal residence (TDM) ages. *Precambrian Research* 127, 287-
794 327.
- 795 Van Schmus, W.R., Oliveira, E.P., Silva Filho, A.F., Toteu, F., Penaye, J., Guimarães,
796 I.P., 2008. Proterozoic links between the Borborema Province, NE Brazil, and the
797 Central African Fold Belt. *Geological Society of London Special Publication* 294, 66-
798 69.
- 799 Vauchez, A., Egydio-Silva, M. 1992. Termination of a Continental-Scale-Strike-Slip
800 Fault in partially melted crust: The West-Pernambuco Shear Zone, Northeast Brazil.
801 *Geology* 20, 1007-1010.
- 802 Vauchez, A., Neves, S.P., Caby, R., Corsini, M., Egydio-Silva, M., Arthaud, M.,
803 Amaro, V.E., 1995. The Borborema shear zone system, NE Brazil. *Journal of South*
804 *American Earth Sciences* 8, 247-266.
- 805 Viegas, L.G., Archanjo, C.J., Hollanda, M.H.B.M., Vauchez, A., 2014. Microfabrics
806 and zircon U-Pb (SHRIMP) chronology of mylonites from the Patos shear zone
807 (Borborema Province, NE Brazil). *Precambrian Research* 243, 1-17.
- 808 Weinberg, R.F., Sial, A.N., Mariano, G., 2004. Close spatial relationship between
809 plutons and shear zones. *Geological Society of America Bulletin* 32, 377-380.

810

811 **FIGURE CAPTIONS**

812 Fig. 1 - a) Pre-drift reconstruction of Northeast South America and West Africa in
813 Western Gondwana context with the main structural provinces and lineaments on its
814 current position. SJCT = São José do Caianho Terrane, PABT = Piancó Alto-Brigida
815 Terrane, APT = Alto Pajeú Terrane, AMT = Alto Moxotó Terrane, RCT = Rio
816 Capibaribe Terrane, TBL = Transbrasiliano Lineament, KL - Khandi Lineament, PaL =
817 Patos Lineament, GAL = Garoua Lineament, PeL = Pernambuco Lineament, AL =
818 Adamoua Lineament.

819 Fig. 2 - Geological map of the study area. Ediacaran granitic suites: I = Serra do
820 Arapuá, II = Riacho do Icó, III - Quixaba, IV = Fortuna. Terranes: APT = Alto Pajeú,
821 AMT = Alto Moxotó, PEALT = Pernambuco Alagoas. JB = Jatobá Basin. The thicker
822 black lines corresponds to the proposed geological Terrane boundaries.

823 Fig. 3 - Covered area by the Pernambuco-Paraíba and Paraíba-Rio Grande do Norte
824 geophysical projects from Brazilian Geological Survey in NE Brazil, with a satellite
825 image of the study area. The thick black dashed line represents the terrane boundaries.

826 Fig. 4 – Gamma-ray spectrometric products of the study area: a) Ternary RGB
827 composition map; b) map of interpreted radiometric domains. Such domains are defined
828 by contrasting signatures on the total count map. The thick yellow dashed line
829 represents the geophysical terrane boundaries. The same is displayed in Figs. 5 to 7.

830 Fig. 5 – Gamma-ray spectrometric maps as well as the main proposed terrane
831 boundaries (thick black dashed lines): a) Total count ($\mu\text{R/h}$); b) eTh/K ratio. c) and d)
832 corresponds to structural interpretations of a) and b) respectively. The thick red lines
833 represent the major radiometric lineaments, whereas the blue lines correspond to
834 secondary lineaments on c) and d). The same is displayed in Figs. 6 to 8.

835 Fig. 6 - Magnetic maps: a) Magnetic anomaly and b) Total Gradient. c) and d)
836 corresponds to structural interpretations of a) and b) respectively.

837 Fig. 7 - Magnetic products: a) First vertical derivate and b) Tilt derivate maps. Note the
838 splay termination of shear zones between the studied terranes as well as sigmoid shapes
839 imposed by the intercalation of magnetic structures. c) and d) corresponds to structural
840 interpretations of a) and b) respectively. The black boxes represent regional structures
841 revealed by geophysics: on a) - The splay termination of terrane boundaries and b)
842 major sigmoid formed in response to conjugated pairs of strike-slip shear zones.

843 Fig. 8 - Interpreted magnetic domains and main magnetic lineaments for the study area.
844 The different magnetic domains were interpreted based on gradient, relief and
845 orientation of first order and second order lineaments.

846 Fig. 9 - 3D Euler deconvolution for the study area for structural index 1. PeL =
847 Pernambuco Lineament, SJSZ = Serra de Jabitacá Shear zone.

848 Fig. 10 - Integrated geophysical and geological data for the main structures of the study
849 area. PSSZ = Poço do Salgueiro shear zone; CSZ = Carqueja shear zone; AISZ =
850 Afogados da Ingazeira Shear zone; SPAZ = Santa Paula Shear Zone; LDZ = Lagoa do
851 Defunto Shear Zone; SPSZ = São Pedro Shear Zone; BFSZ = Barra da Forquilha Shear
852 Zone; RQ = Riacho Quixaba Shear Zone; SJSZ = Serra de Jabitacá Shear Zone; FSZ =
853 Floresta Shear Zone; AISZ = Airí Shear Zone; RJSZ = Riacho Jacaré Shear Zone; PeL =
854 Pernambuco Lineament; PASZ = Poço da Areia Shear Zone; RBSZ = Riacho do Buraco
855 Shear Zone; RMSZ = Riacho da Maravilha Shear Zone; IF = Ibimirim Fault.

856 Fig. 11 - Structural map of the study area with schematic geological sections and
857 synthetic contour plots stereograms (lower hemisphere Schmidt projections). Structures
858 label are as in Fig. 10.

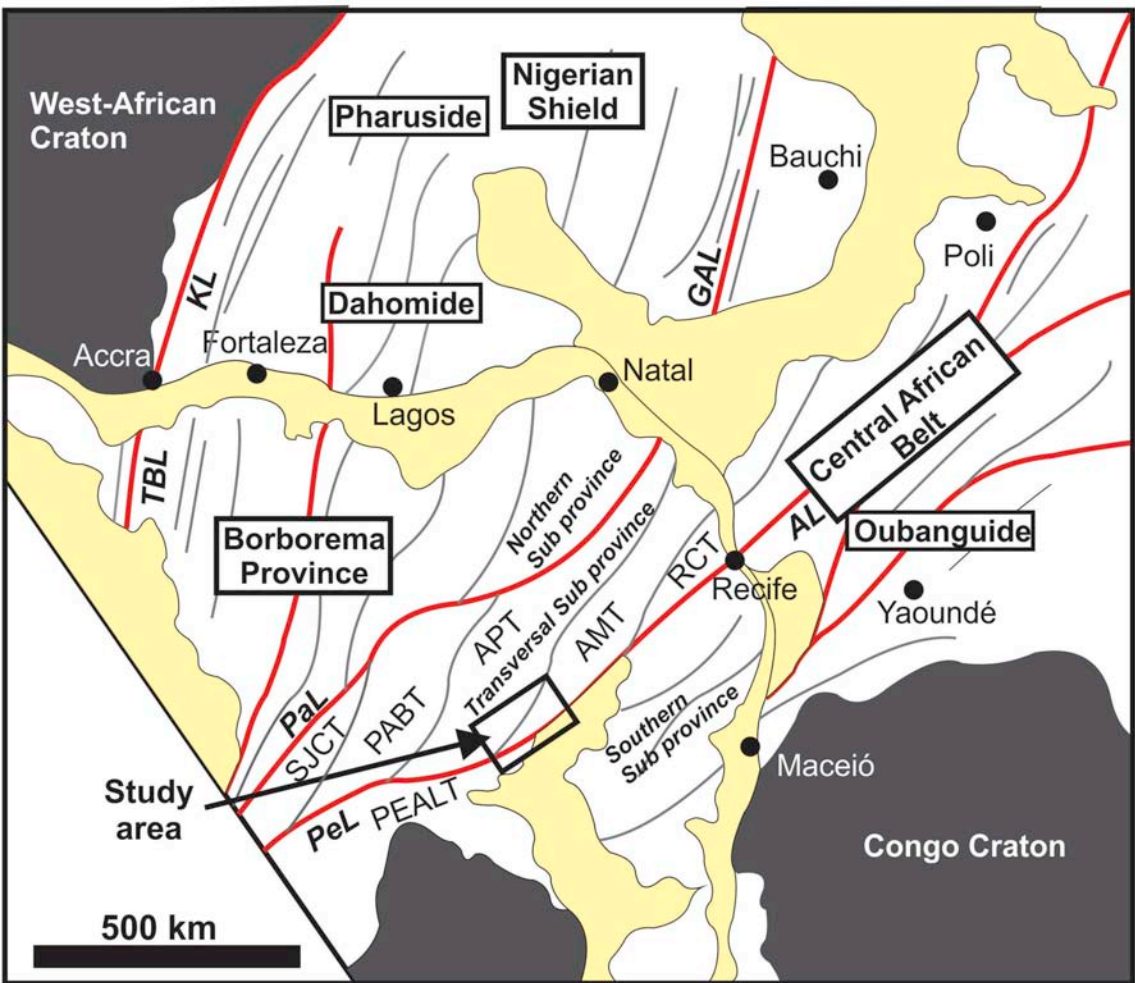
859 Fig. 12 - Structural markers related to D_n and D_{n+1} phases. a) Stromatic to folded
860 migmatite of the ca. 2.6 Ga Riacho das Lajes Suite exhibiting relict S_n foliation
861 (intrafolial fold) in a metatexitic facies; b) strongly mobilized diatexite of the Riacho
862 das Lajes Suite showing schollen structure associated with mafic facies; c) gently
863 dipping S_{n+1} foliation in tabular sheet of Cariris Velhos metagranitoid of the Alto Pajeú
864 Terrane; d) High pitch L_{n+1} mineral stretching lineation on fine-grained Tonian (ca. 0.92
865 Ga) metagranitoid.

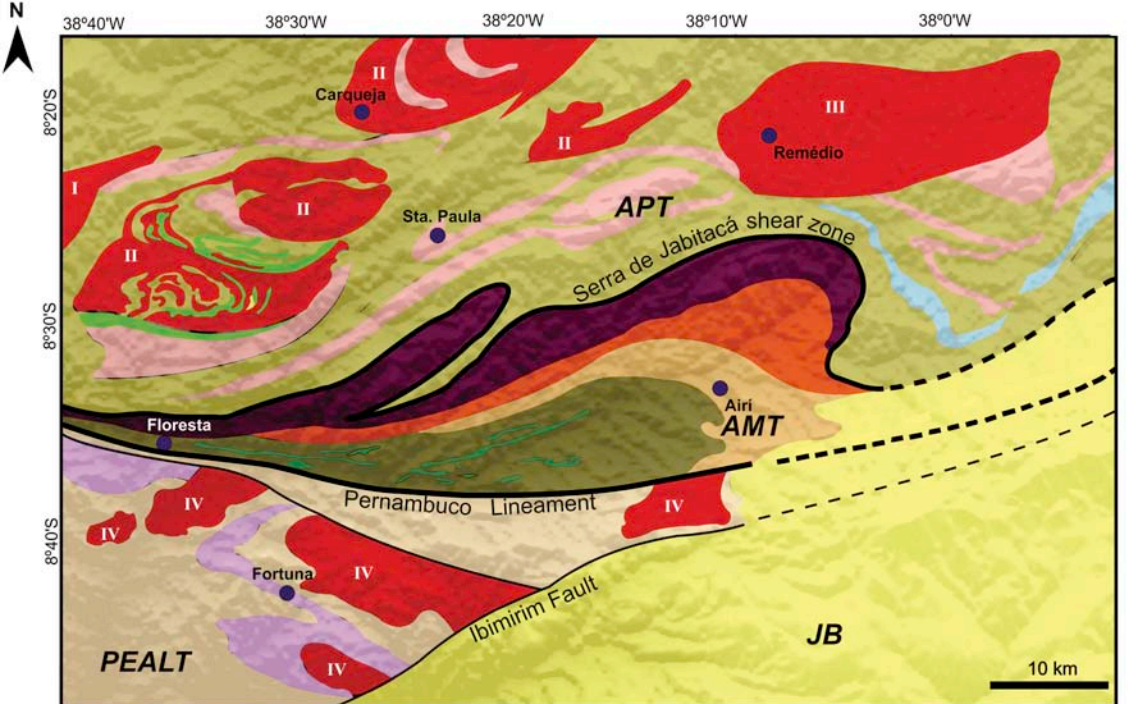
866 Fig. 13 - Structural markers related to D_{n+2} phase D_{n+1} phases. a) F_{n+1} ptygmatic folds
867 indicating distinct competency between leucocratic and mesocratic materials; b)
868 $8^\circ/360Az$ dipping S_{n+1} mylonitic fabrics in a linear tectonite of the ca. 0.97 Ga São
869 Caetano Complex, with associated asymmetric porphyroclasts suggesting top-to-the-S
870 thrust vergence; c) quartz ribbons with undulose extinction in a recrystallized quartz
871 matrix in protomylonitic rock; d) mica fish developed in a mylonitic facies of the São
872 Caetano Complex associated with the Serra de Jabitacá Shear Zone, exhibiting
873 clockwise movement.

874 Fig. 14 - Structural markers related to D_{n+2} phase. a) Banded orthogneiss of the ca. 2.1
875 Ga Floresta Suite displaying deformed leuco- and mesocratic E-W bends; b) horizontal
876 L_{n+2} stretching mineral lineation associated to a vertical S_{n+2} foliation plane of the
877 Pernambuco Lineament; c) photomicrograph of granodioritic mylonite with mica fish
878 arranged between C-type shear bands associated with the Pernambuco Lineament; d)
879 oblique L_{n+2} lineation in mylonitic paragneiss of the ca. 2.01 Ga Sertânia Complex
880 related to the Pernambuco Lineament.

881 Fig. 15 - Structural markers related to a) D_{n+3} Conjugated pair of fractures forming
882 domino-like structures of deformation cross-cutting S_{n+2} foliation planes in paragneiss
883 of the ca. 0.97 Ga São Caetano Complex; b) Detail of collected sample from fracture
884 plane in a), showing neo-formed greenish mineral aggregates (probably quartz, chlorite
885 and sericite).

886 Fig. 16 - Structural model for terrane collage between the studied terranes. Terranes -
887 AMT - Alto Moxotó, APT = Alto Pajeú, RCT = Rio Capibaribe, PEALT = Pernambuco
888 Alagoas. Shear zones - RBSZ = Riacho do Boi, PASZ = Poço da Areia, PL =
889 Pernambuco Lineament, ASZ = Airí, FSZ = Floresta, SJSZ = Serra de Jabitacá, BFSZ =
890 Barra da Forquilha, AISZ = Afogados da Ingazeira. TB = Terrane boundary.





Phanerozoic - Sedimentary cover

Yellow Sandstones and pelitic rocks (Jatobá Basin)

Meso-Neoproterozoic - Alto Pajeú and Pernambuco-Alagoas terranes (1000 - 600 Ma)

Red Brasiliano-related granites and granodiorites (Suites I to IV)

Pink Cariris Velhos metagranitoids

Green Metagabbros, metapyroxenites and metaperidotites (Serrote das Pedras Pretas Suite)

Light green Bioite-muscovite paragneisses, quartzites and volcanoclastic rocks (São Caetano Complex)

Purple Paragneisses, biotite-schists and marbles (Cabrobró Complex)

Light yellow Orthogneisses, migmatites and aphanolites (Belém do São Francisco Complex)

Paleoproterozoic - Alto Moxotó Terrane (2100 - 1600 Ma)

Dark purple Augen gneisses and metagranites (Riacho do Navio Suite)

Dark green Metagabbros and metapyroxenites (Malhada Vermelha Suite)

Orange Garnet-sillimanite-biotite paragneisses and migmatites (Sertânia Complex)

Olive green Metadiorites, metatonalites and metagranodiorites (Floresta Suite)

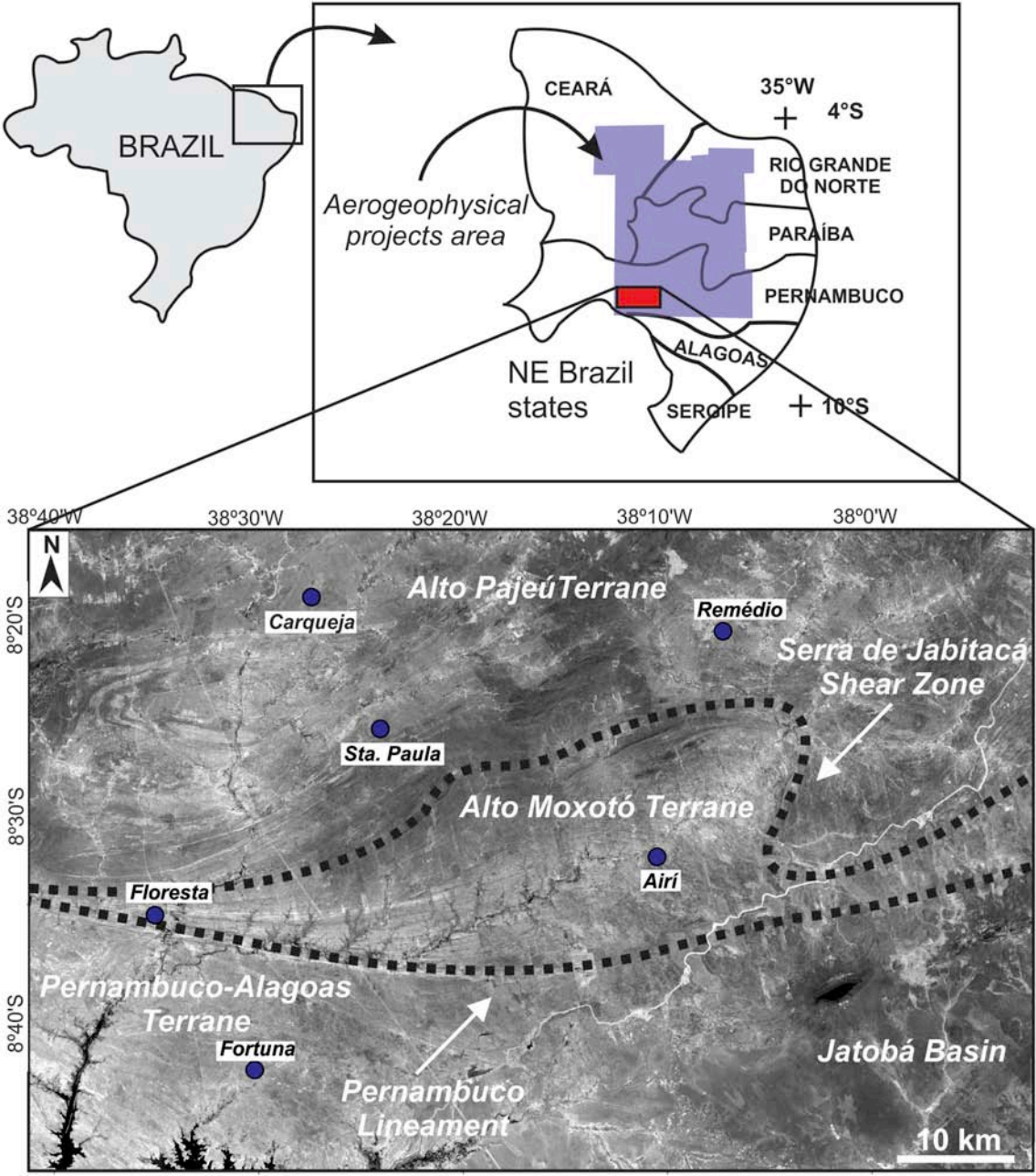
Archean - Alto Moxotó Terrane (2600 Ma)

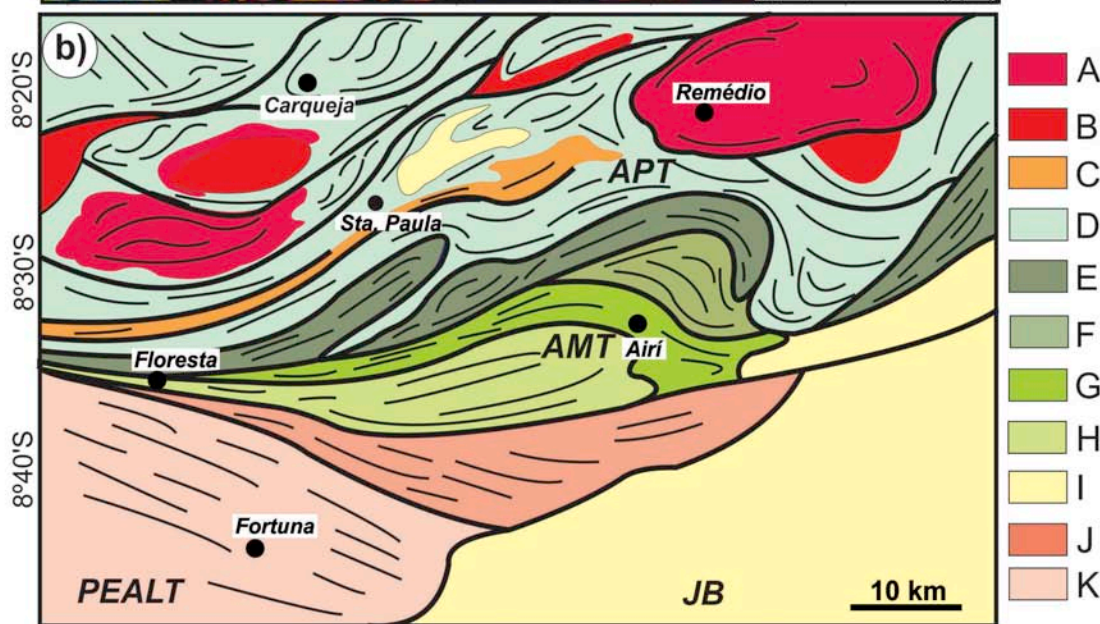
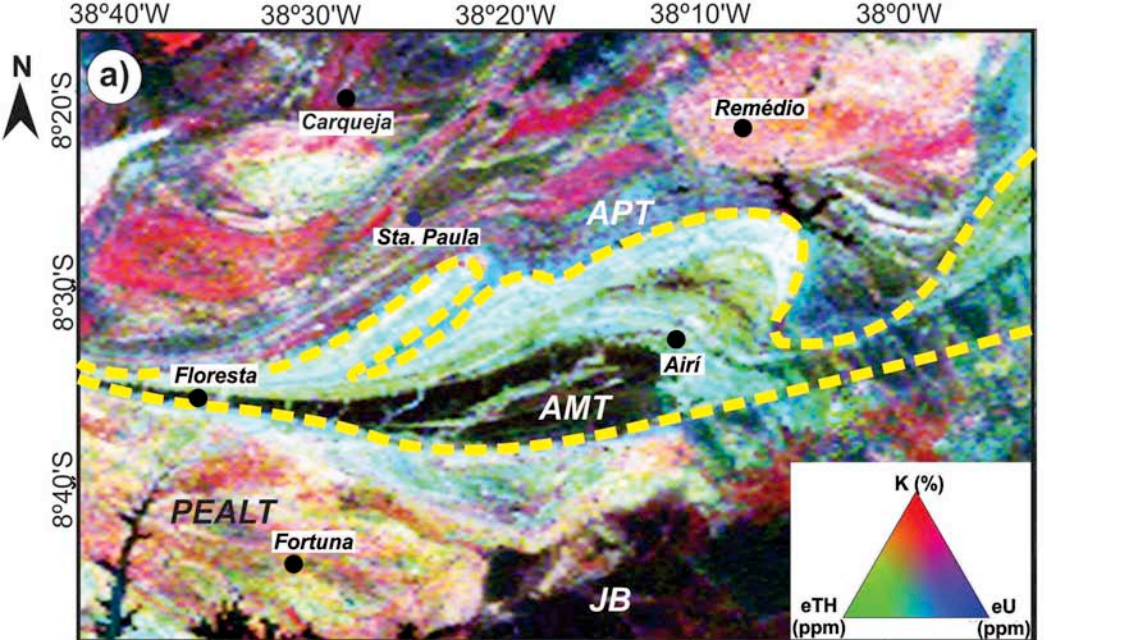
Light orange Metatonalites, metatrandhjemites and metagranodiorites (Riacho das Lajes Suite)

Solid line Main structures

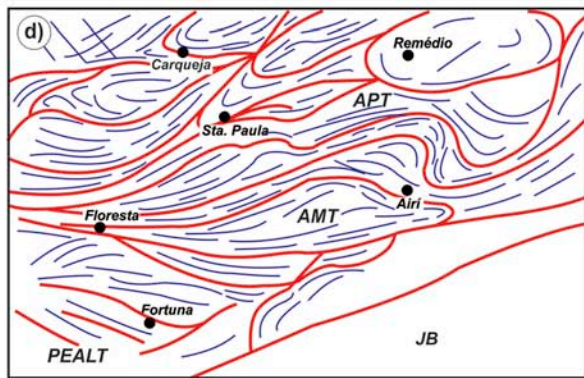
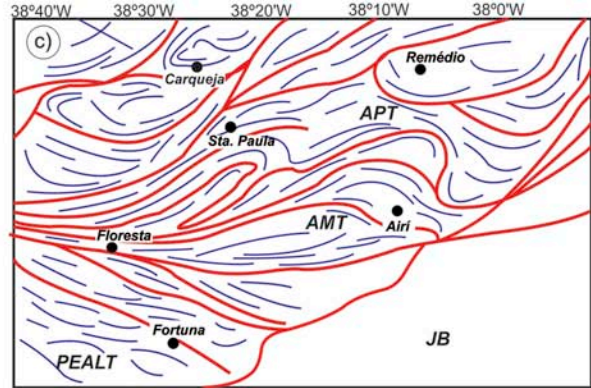
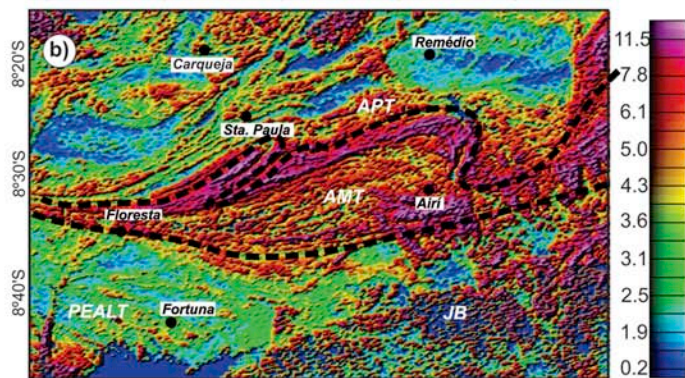
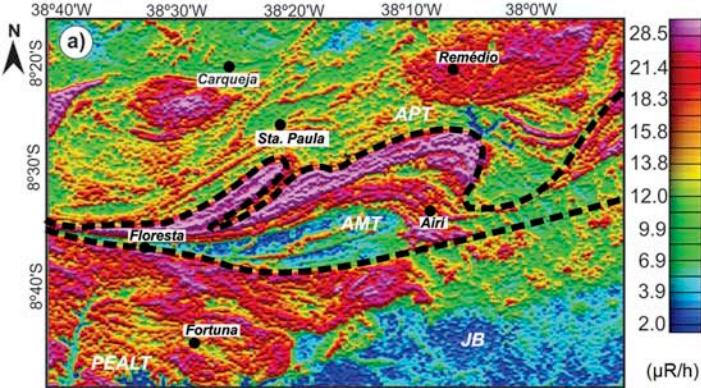
Dashed line Covered structures

Blue dot Towns and minor locations

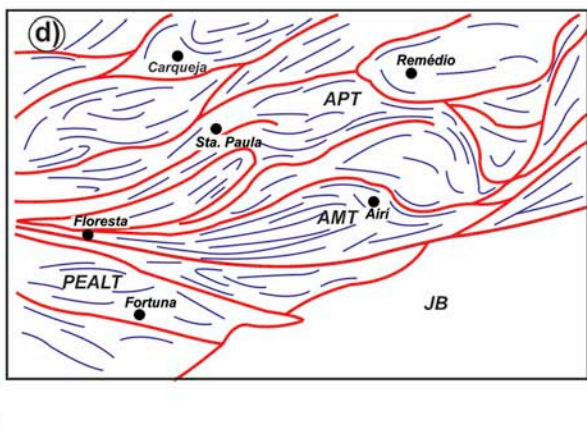
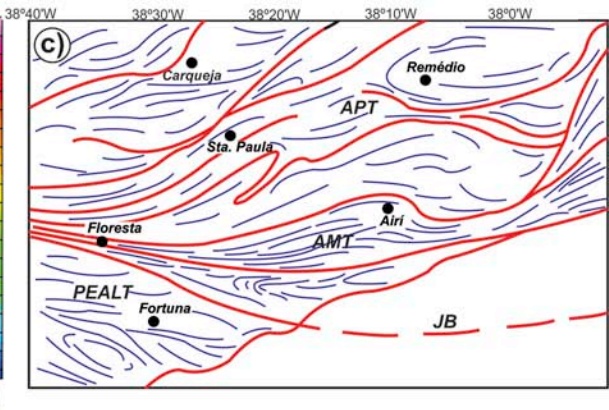
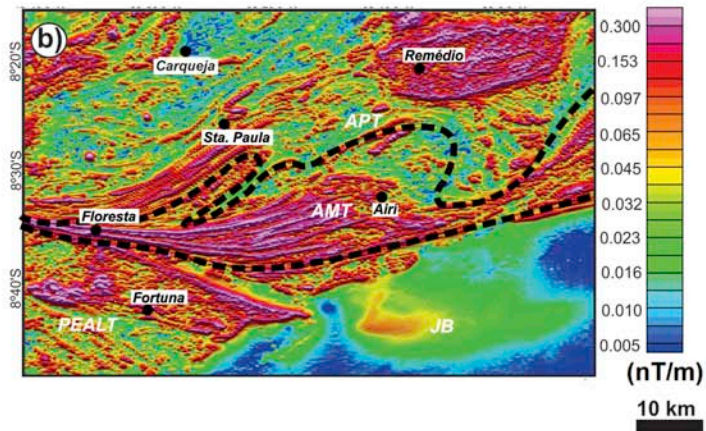
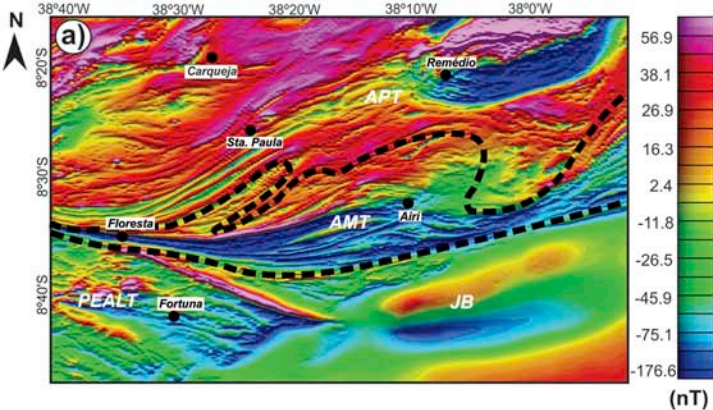




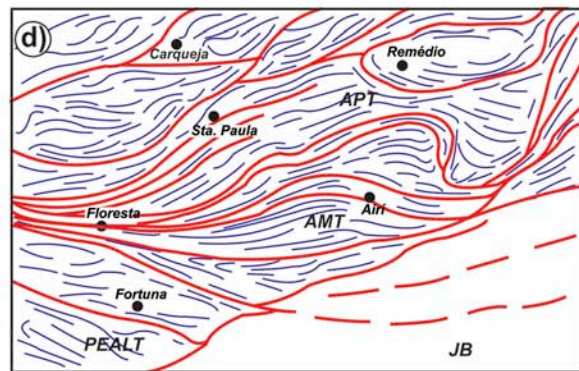
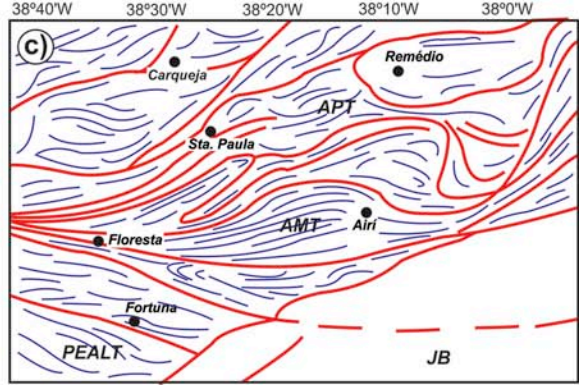
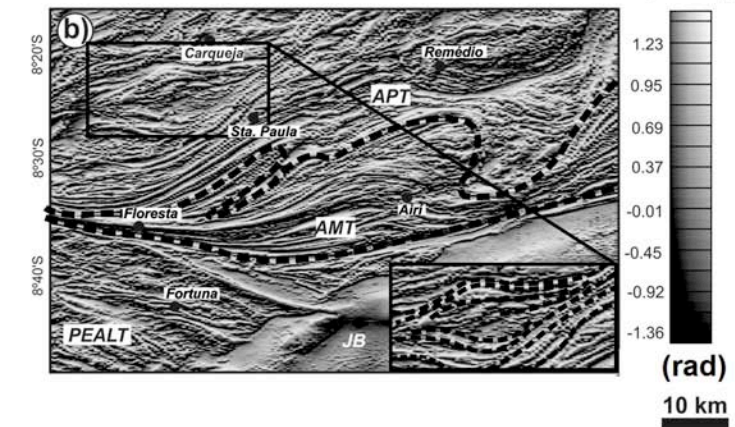
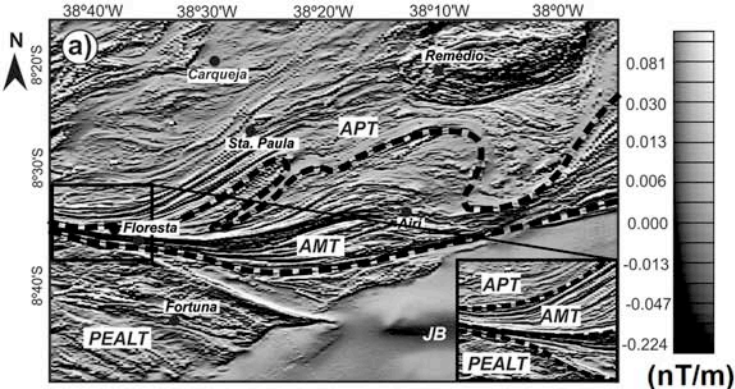
Major radiometric lineaments / Secondary radiometric lineaments

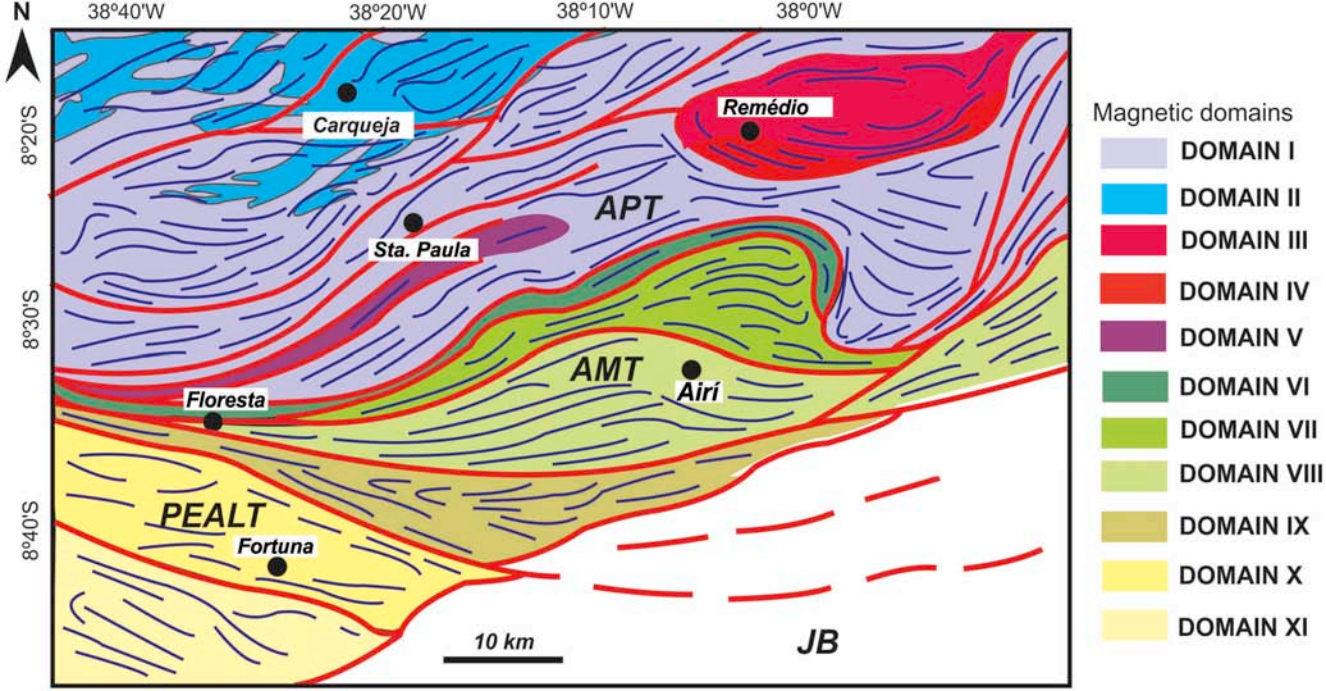


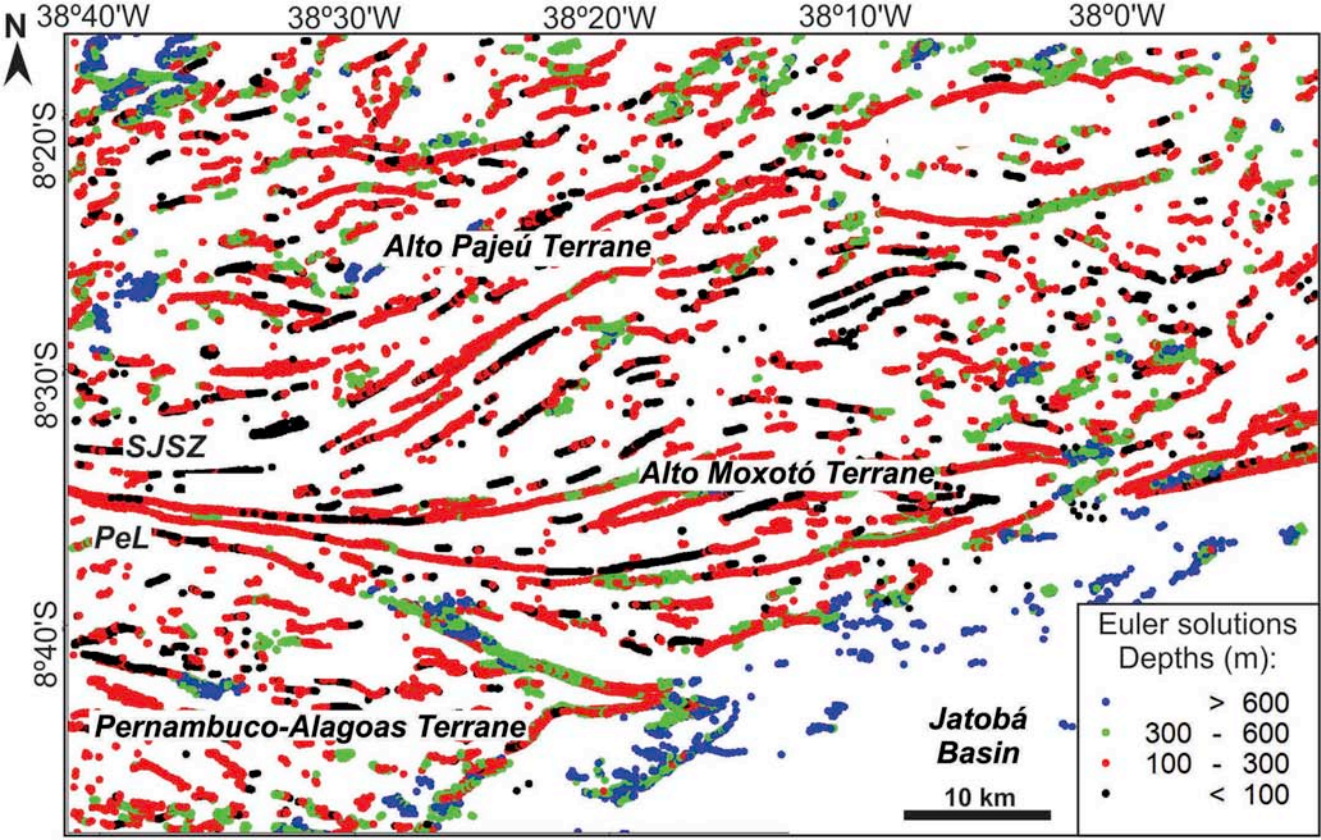
10 km

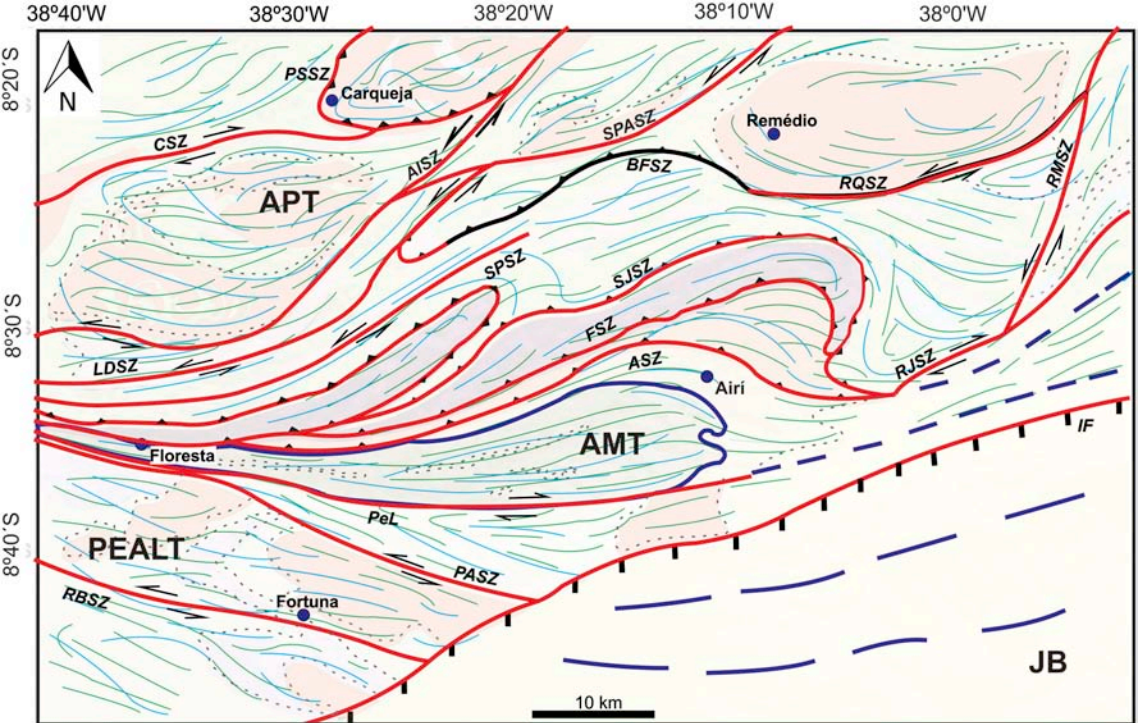


10 km

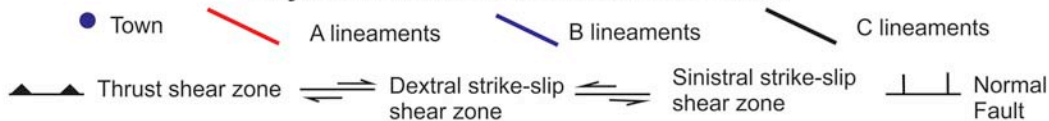




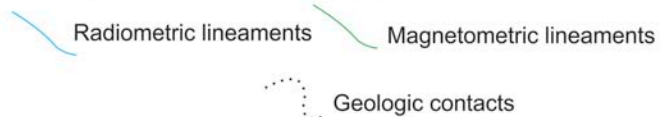


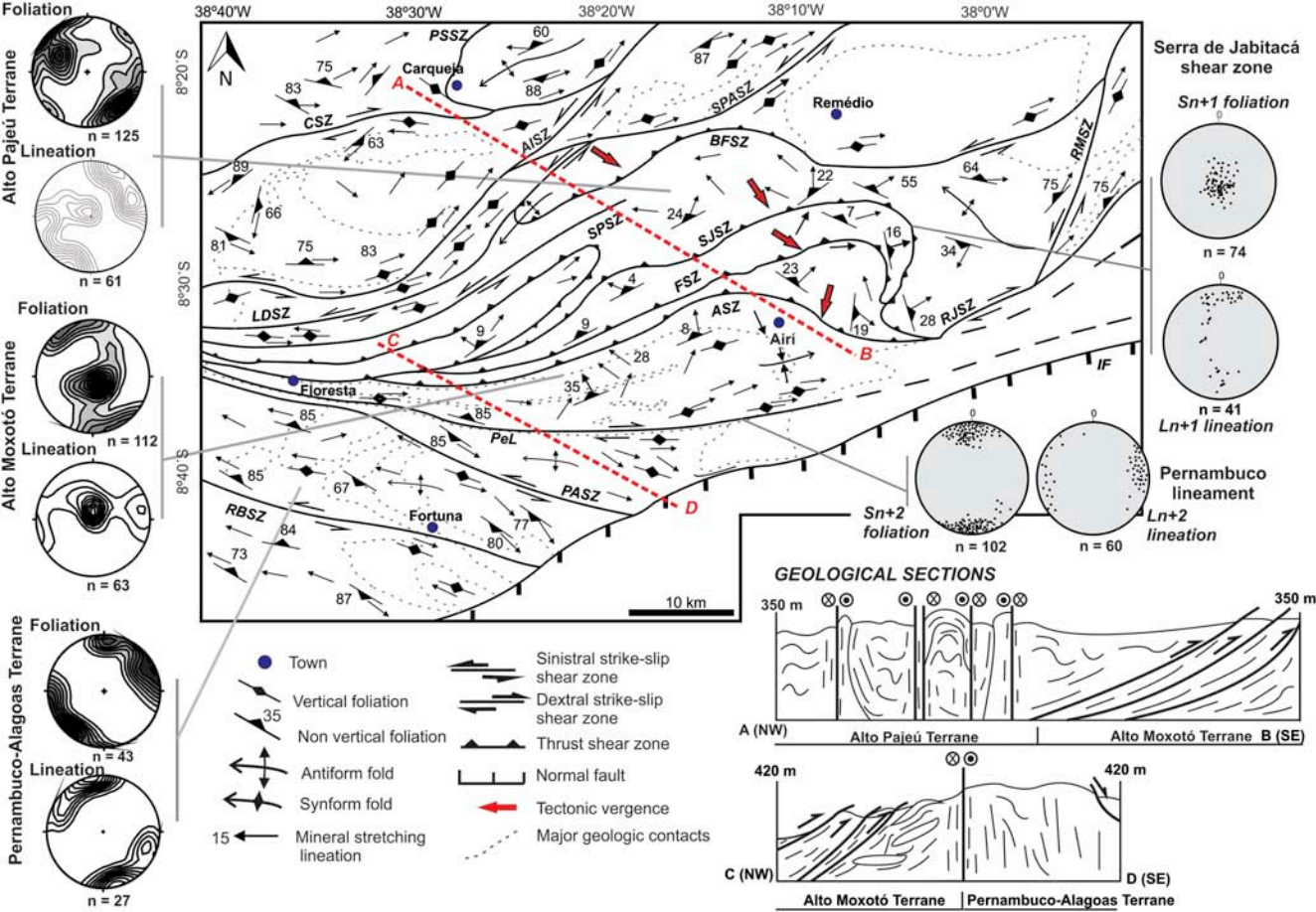


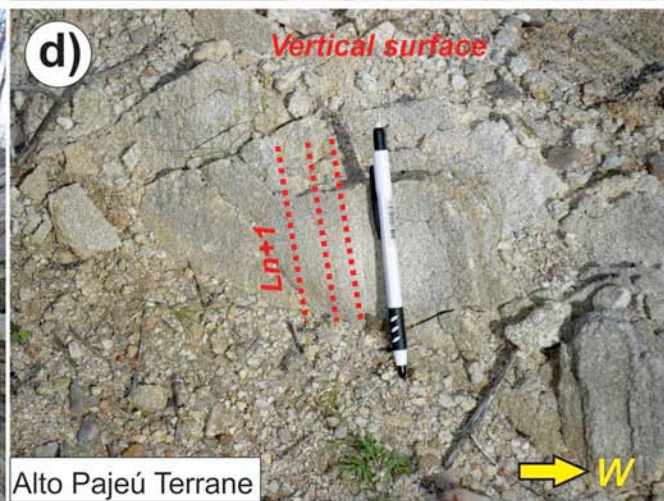
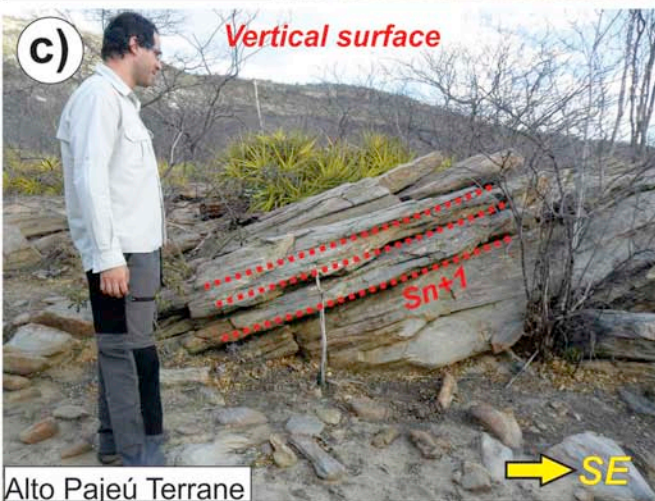
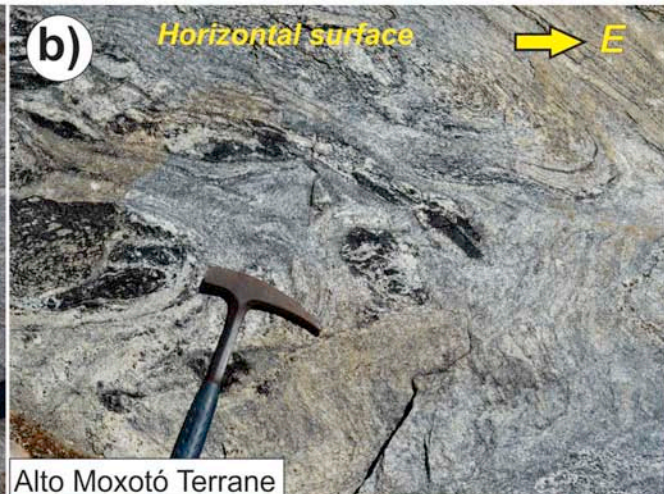
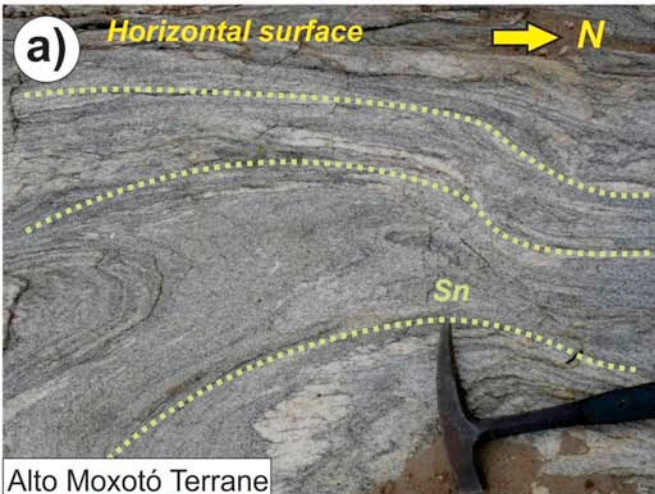
Major Lineaments and structure kinematics

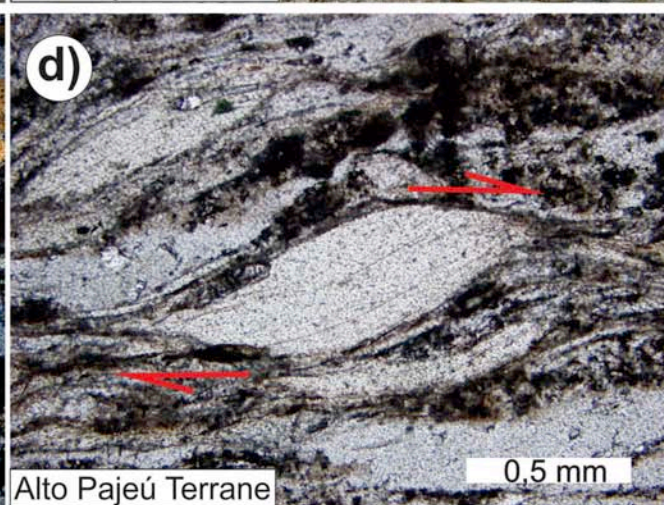
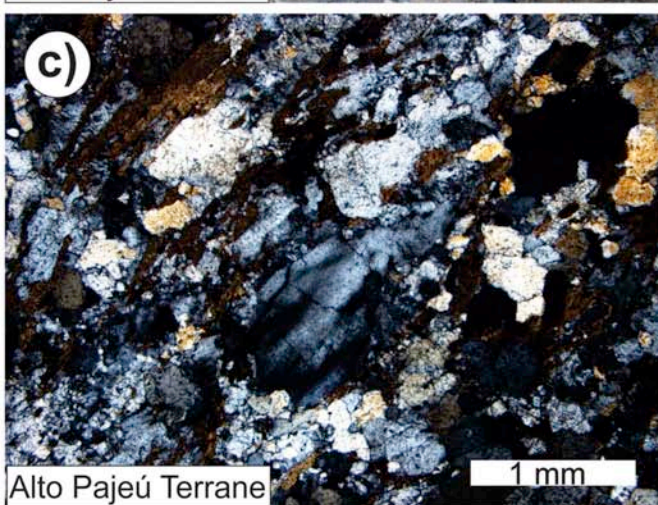
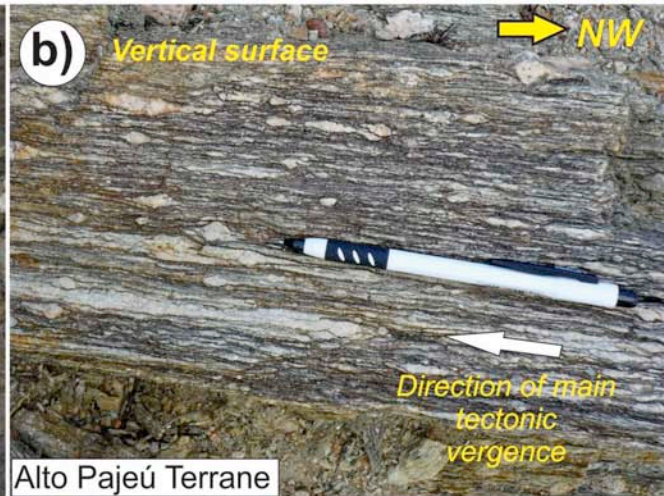
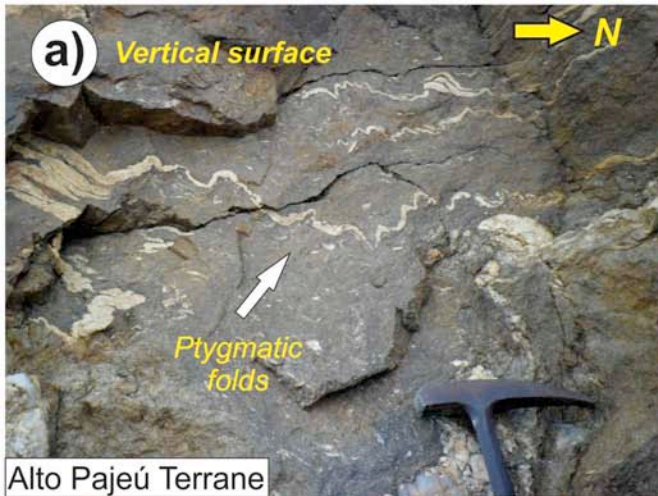


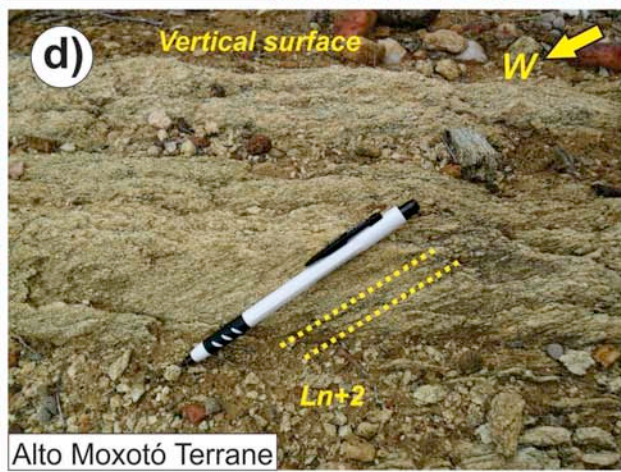
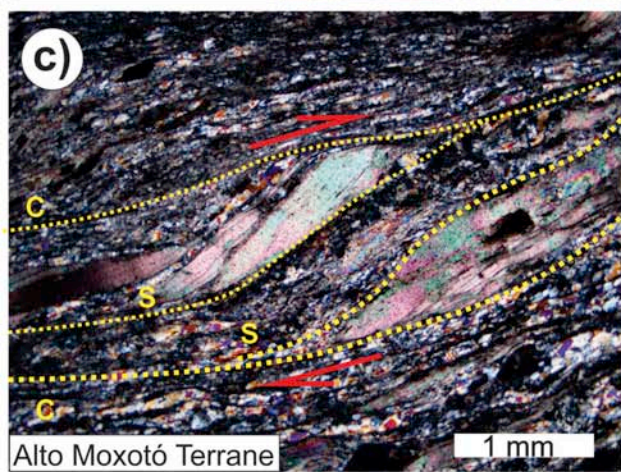
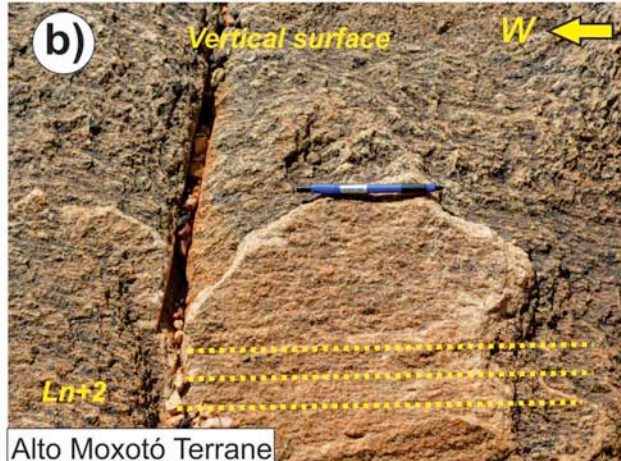
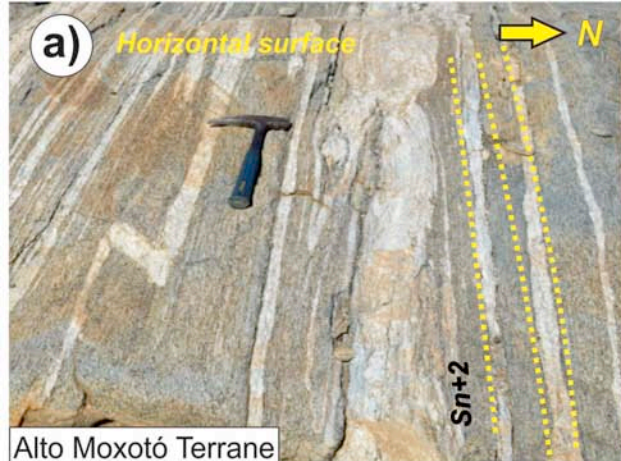
Compilation of secondary geophysical lineaments



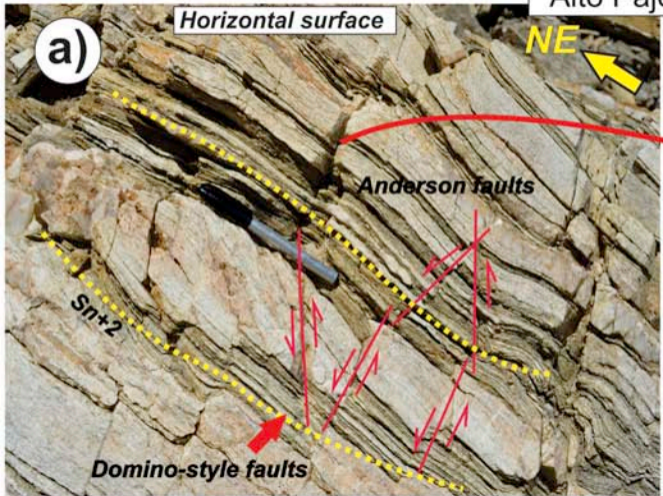




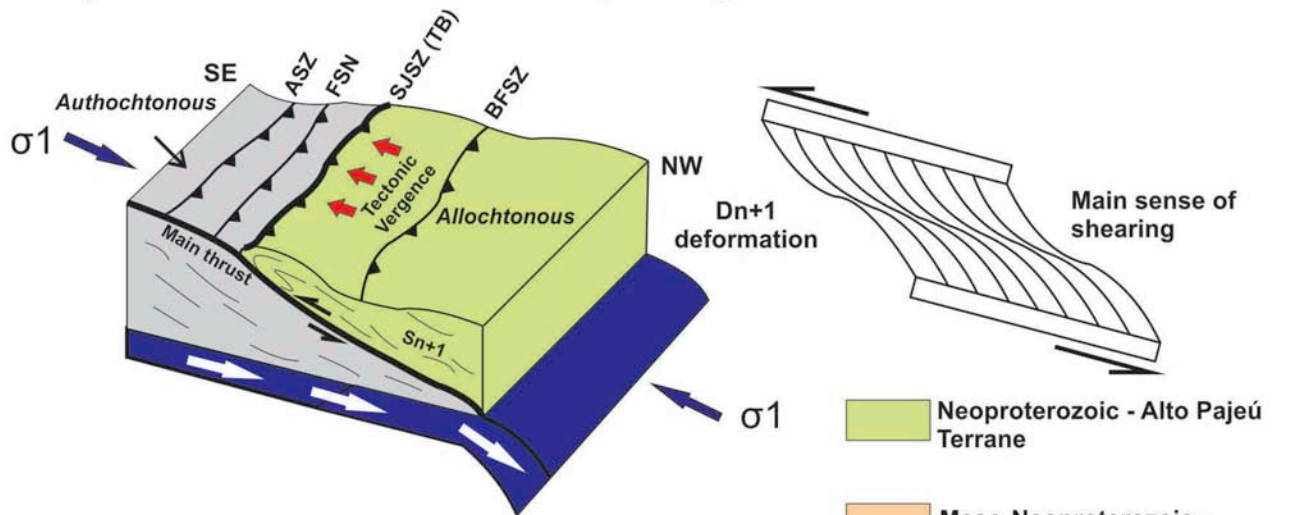




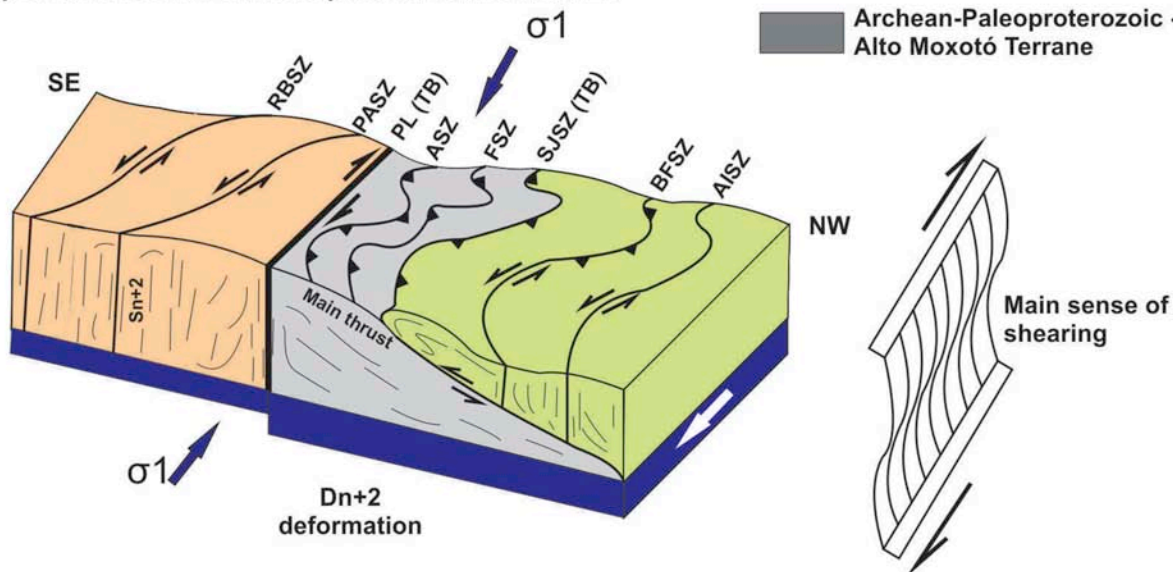
Alto Pajeú Terrane



a) Stage 1 - Tonian or Early Ediacaran: APT-AMT composite frontal/oblique assembly in response to Thick Skinned Tectonics developed through the SJSZ



b) Stage 2 - Ediacaran-Cambrian: APT-AMT-PEALT lateral assembly in response to Dextral Strike-slip Movement of the PEL



Highlights

- > Combined geophysical and structural data highlight the tectonic evolution of the central portion of the Borborema Province in NE Brazil;
- > Polyphase deformation suggest two distinct events of collage via frontal/oblique and lateral terrane boundaries;
- > According to our model, the Borborema Province was affected by accretionary orogenesis during the Neoproterozoic;
- > Our results provide new insights on the crustal evolution of Western Gondwana inner orogens.